REPORT

De Novo Disruption of the Proteasome Regulatory Subunit *PSMD12* Causes a Syndromic Neurodevelopmental Disorder

Sébastien Küry,[1] Thomas Besnard,[1] Frédéric Ebstein,[2] Tahir N. Khan,[3] Tomasz Gambin,[4,5,6] Jessica Douglas,[7] Carlos A. Bacino,[4,8] Stephan J. Sanders,[9] Andrea Lehmann,[2] Xénia Latypova,[1] Kamal Khan,[3] Mathilde Pacault,[1] Stephanie Sacharow,[7] Kimberly Glaser,[10] Eric Bieth,[11] Laurence Perrin-Sabourin,[12] Marie-Line Jacquemont,[13] Megan T. Cho,[14] Elizabeth Roeder,[4,15] Anne-Sophie Denommé-Pichon,[16] Kristin G. Monaghan,[14] Bo Yuan,[4,8] Fan Xia,[4,8] Sylvain Simon,[17,18,19] Dominique Bonneau,[16,20] Philippe Parent,[21] Brigitte Gilbert-Dussardier,[22,23] Sylvie Odent,[24,25] Annick Toutain,[26,27] Laurent Pasquier,[24,25] Deborah Barbouth,[10] Chad A. Shaw,[4,8] Ankita Patel,[4,8] Janice L. Smith,[4,8] Weimin Bi,[4,8] Sébastien Schmitt,[1] Wallid Deb,[1] Mathilde Nizon,[1] Sandra Mercier,[1] Marie Vincent,[1] Caroline Rooryck,[28] Valérie Malan,[29] Ignacio Briceño,[30] Alberto Gómez,[30] Kimberly M. Nugent,[15] James B. Gibson,[31] Benjamin Cogné,[1] James R. Lupski,[4,32,33] Holly A.F. Stessman,[34] Evan E. Eichler,[34,35] Kyle Retterer,[14] Yaping Yang,[4,8] Richard Redon,[36,37] Nicholas Katsanis,[3,38] Jill A. Rosenfeld,[4] Peter-Michael Kloetzel,[2] Christelle Golzio,[3] Stéphane Bézieau,[1,17] Paweł Stankiewicz,[4,8,39,40,*] and Bertrand Isidor[1,40,*]

Degradation of proteins by the ubiquitin-proteasome system (UPS) is an essential biological process in the development of eukaryotic organisms. Dysregulation of this mechanism leads to numerous human neurodegenerative or neurodevelopmental disorders. Through a multi-center collaboration, we identified six de novo genomic deletions and four de novo point mutations involving *PSMD12*, encoding the non-ATPase subunit PSMD12 (aka RPN5) of the 19S regulator of 26S proteasome complex, in unrelated individuals with intellectual disability, congenital malformations, ophthalmologic anomalies, feeding difficulties, deafness, and subtle dysmorphic facial features. We observed reduced PSMD12 levels and an accumulation of ubiquitinated proteins without any impairment of proteasome catalytic activity. Our *PSMD12* loss-of-function zebrafish CRISPR/Cas9 model exhibited microcephaly, decreased convolution of the renal tubules, and abnormal craniofacial morphology. Our data support the biological importance of PSMD12 as a scaffolding subunit in proteasome function during development and neurogenesis in particular; they enable the definition of a neurodevelopmental disorder due to *PSMD12* variants, expanding the phenotypic spectrum of UPS-dependent disorders.

Proteolysis by the ubiquitin-proteasome system (UPS) is a tightly regulated biological process in eukaryotic cells and is crucial for their homeostasis, signaling, and fate determination.[1–3] Proteins subjected to degradation are typically marked by polyubiquitin chains to be hydrolyzed in a precise, rapid, timely, and ATP-dependent manner by the 19S regulatory subunit of the 26S proteasome.[3–6] UPS-dependent degradation essentially contributes to proteostasis and plays a key role in neuronal development and function[7,8] by regulating synaptic plasticity,[9,10]

[1]Service de Génétique Médicale, CHU de Nantes, 9 quai Moncousu, 44093 Nantes Cedex 1, France; [2]Institute of Biochemistry, Charité Universitätsmedizin Berlin, Charité Platz 1/Virchowweg 6, 10117 Berlin, Germany; [3]Center for Human Disease Modeling, Duke University Medical Center, Durham, NC 27710, USA; [4]Department of Molecular and Human Genetics, Baylor College of Medicine, Houston, TX 77030, USA; [5]Institute of Computer Science, Warsaw University of Technology, Warsaw 00-661, Poland; [6]Department of Medical Genetics, Institute of Mother and Child, Warsaw 01-211, Poland; [7]Division of Genetics and Genomics, Boston Children's Hospital and Harvard Medical School, Boston, MA 02115, USA; [8]Baylor Genetics, Houston TX, 77030, USA; [9]Department of Psychiatry, Weill Institute for Neurosciences, University of California, San Francisco, San Francisco, CA 94158, USA; [10]Dr. John T. Macdonald Foundation Department of Human Genetics, Miller School of Medicine, University of Miami, Miami, FL 33136, USA; [11]Service de Génétique Médicale, Hôpital Purpan, CHU de Toulouse, 31059 Toulouse, France; [12]Fédération de Génétique, Hôpital Robert Debré, Assistance Publique – Hôpitaux de Paris, 75935 Paris Cedex 19, France; [13]Génétique Médicale, CHU de La Réunion, 97448 Saint Pierre, La Réunion, France; [14]GeneDx, Gaithersburg, MD 20877, USA; [15]Department of Pediatrics, Baylor College of Medicine, San Antonio, TX 78207, USA; [16]Département de Biochimie et Génétique, CHU d'Angers, 49933 Angers Cedex 9, France; [17]Centre de Recherche en Cancérologie et Immunologie Nantes-Angers, INSERM, Université d'Angers et Université de Nantes, 44007 Nantes, France; [18]LabEx "Immunotherapy, Graft, Oncology," 44093 Nantes, France; [19]Department of Dermato-cancerology, CHU de Nantes, 44093 Nantes, France; [20]INSERM UMR 1083, CNRS UMR 6214, 49933 Angers Cedex 9, France; [21]Génétique Médicale, CHRU de Brest, 29609 Brest, France; [22]Service de Génétique, CHU de Poitiers, BP 577, 86021 Poitiers, France; [23]Equipe d'Accueil 3808, Université de Poitiers, 86022 Poitiers Cedex, France; [24]Service de Génétique Clinique, Centre Hospitalier Universitaire de Rennes, 35203 Rennes, France; [25]CNRS UMR 6290, Université de Rennes 1, 2 Avenue du Professeur Léon Bernard, 35043 Rennes, France; [26]Service de Génétique, CHU de Tours, 2 Boulevard Tonnellé, 37044 Tours, France; [27]INSERM UMR U930, Faculté de Médecine, Université François Rabelais, 37044 Tours, France; [28]Service de Génétique Médicale, CHU de Bordeaux, 33076 Bordeaux, France; [29]Service d'Histologie-Embryologie-Cytogénétique, Hôpital Necker-Enfants Malades, Assistance Publique – Hôpitaux de Paris, 75015 Paris, France; [30]Instituto de Genética Humana, Facultad de Medicina, Pontificia Universidad Javeriana, 110231 Bogotá, Colombia; [31]Clinical and Metabolic Genetics, 'Specially for Children, Austin, TX 78723, USA; [32]Department of Pediatrics, Texas Children's Hospital, Houston, TX 77030, USA; [33]Human Genome Sequencing Center, Baylor College of Medicine, Houston, TX 77030, USA; [34]Department of Genome Sciences, University of Washington School of Medicine, Seattle, WA 98195, USA; [35]Howard Hughes Medical Institute, Seattle, WA 98195, USA; [36]INSERM, CNRS, l'Institut du Thorax, Université de Nantes, 44007 Nantes, France; [37]L'Institut du Thorax, CHU de Nantes, 44093 Nantes, France; [38]Department of Cell Biology, Duke University Medical Center, Durham, NC 27710, USA; [39]Institute of Mother and Child, Warsaw 01-211, Poland
[40]These authors equally contributed to this work
*Correspondence: pawels@bcm.edu (P.S.), bertrand.isidor@chu-nantes.fr (B.I.)
http://dx.doi.org/10.1016/j.ajhg.2017.01.003.

Table 1. Clinical Features of the Subjects with De Novo Point Mutations and CNV Deletions Involving *PSMD12*

	Subject 1	Subject 2	Subject 3	Subject 4	Subject 5	Subject 6	Subject 7	Subject 8	Subject 9	Subject 10
Center of enrollment	HUGODIMS	BCH	SSC	BG	BG	BG	CHU de Toulouse	CHU de la Réunion	BG	BG
PSMD12 variant[a]	c.367C>T (p.Arg123*)	c.1274 T>G (p.Leu425*)	c.601C>T (p.Arg201*)	c.909−2A>G (p.?)	deletion	deletion	deletion	deletion	deletion	deletion
Size of deletion (Mb)	–	–	–	–	1.37	4.06	1.46	1.24	0.84	0.62 (complex)
Deletion proximal breakpoints[b]	–	–	–	–	64,585,784–64,598,722	62,280,810–62,289,975	64,529,282–64,590,936	64,461,987–64,529,223	65,319,589	65,090,765
Deletion distal breakpoints[b]	–	–	–	–	65,972,166–66,162,742	66,352,008–66,398,204	65,955,949–65,989,022	65,720,329–65,766,756	66,162,742	65,711,757
Gender	male	male	male	male	female	male	male	female	female	female
Age at assessment	8 y, 4 m	10 y, 7 m	14 y, 8 m	14 y, 10 m	21 m	3 y, 6 m	13 y, 2 m	5 y, 11 m	4 y, 6 m	9 y
Weight (g) at birth (SD)	2,500 (−2)	2,466 (−2)	3,033 (−0.84)	3,200 (−0.5)	ND	2,390 (−2.2)	1,570 (−4)	2,590 (−1.5)	1,900 (−2.9)	2,100 (−2.5)
Length (cm) at birth (SD)	46 (−2)	43 (−3.5)	48.3 (−0.70)	50 (mean)	ND	47 (−1.5)	44 (−3)	43.5 (−3)	43.2 (−2.8)	46 (−1.55)
OFC (cm) at birth (SD)	36 (+1)	32 (−2)	34.9 (−0.44)	ND	ND	32 (−2)	33.5 (−1)	32 (−2)	30 (−3.3)	ND
Weight (kg) at assessment (SD)	25 (−0.5)	28.6 (−1)	61.7 (+0.60)	42.4 (−1)	ND	11.3 (−2.64)	31 (−2)	16.8 (−1.37)	ND (3rd percentile)	40 (+1.36)
Length (cm) at assessment (SD)	120 (−1)	129.8 (−1.7)	173 (+0.84)	163 (mean)	ND	91 (−2.2)	134 (−2.5)	103.5 (−2.07)	ND (10th–25th percentile)	140 (+1.10)
OFC (cm) at assessment (SD)	52.5 (−0.5)	52 (−1)	57 (+1.48)	ND	ND, microcephaly	47.6 (−1.6)	51.5 (−2)	50 (−0.57)	ND (5th–10th percentile)	55 (+2.32)
Neurological Abnormalities										
Intellectual disability	+	+	+	+	+	+	+	+	+	+
Motor delay	+	+	−	−	+	+	+	−	+	+
Speech delay	+	+	+	−	+	+	+	+	+	+
Abnormal behavior	+	+	+	+	−	ND	+	+	ND	+
Seizures	−	+	−	+	−	−	−	−	−	+
Hypotonia	+	−	ND	+	−	+	+	−	+	+
Deafness	+	+	−	−	−	+	−	−	−	−
Feeding difficulties	+	+	−	−	−	+	+	−	+	−
Brain MRI	normal	normal	ND	abnormal	ND	abnormal	normal	normal	ND	normal
Congenital Malformations										
Cardiac	+	+	+	−	+	+	−	−	−	−
Renal	+	+	−	ND	+	+	−	−	+	+

(*Continued on next page*)

Table 1. *Continued*

	Subject 1	Subject 2	Subject 3	Subject 4	Subject 5	Subject 6	Subject 7	Subject 8	Subject 9	Subject 10
Genital	+	+	+	+	–	+	–	–	–	+
Skeletal	+	+	–	–	–	+	+	–	+	–
Other	–	+	–	–	–	–	–	–	–	–
Craniofacial Abnormalities										
Ophthalmological	+	+	ND	+	+	+	+	–	+	+
Ears	+	+	ND	+	–	+	–	+	+	+
(Micro)retrognathia	+	–	ND	–	+	–	+	–	+	–
Other	–	–	ND	+	+	+	+	+	+	+

More comprehensive information regarding clinical features is cataloged in Table S1. Abbreviations are as follows: y, years; m, months; ND, not determined; SD, standard deviation; OFC, occipito-frontal circumference; MRI, magnetic resonance imaging; CHU, Centre Hospitalier Universitaire; BCH, Boston Children's Hospital; BG, Baylor Genetics Laboratories; and SSC, Simons Simplex Collection.
[a]For SNVs: HGVS nomenclature version 2.0 according to mRNA reference sequence GenBank: NM_002816.3. Nucleotide numbering uses 1 as the initiation codon and +1 as the A of the ATG translation initiation codon in the reference sequence.
[b]Human genome reference: UCSC Genome Browser hg19.

neurotransmitter release via intracellular trafficking,[11,12] and morphogenesis of axons, dendrites, and dendritic spines.[7] Neurons are therefore highly vulnerable to UPS dysfunction, as evidenced by a wide spectrum of neurodegenerative proteinopathies, including polyglutamine disorders (e.g., spinal bulbar muscular atrophy [MIM: 313200] and Huntington disease [MIM: 143100]), Alzheimer disease (MIM: 104300), Parkinson disease (MIM: 168600), and amyotrophic lateral sclerosis (MIM:105400).[13,14] Impairment of UPS activity can also result in neurodevelopmental delay, as exemplified by alterations of ubiquitin ligase genes *UBE3A* (MIM: 601623; associated with Angelman syndrome [MIM: 105830]),[15] *UBE3B* (MIM: 608047; associated with Kaufman oculocerebrofacial syndrome [MIM: 244450]),[16] and *HUWE1* (MIM: 300697; associated with X-linked Turner-type syndromic mental retardation [MIM: 300706])[17] and deubiquitinating enzyme genes *USP7* (MIM: 602519; associated with chromosome 16p13.2 deletion syndrome [MIM: 616863])[18] and *USP9X* (MIM: 300072; associated with mental retardation, X-linked 99 [MIM: 300919] and mental retardation, X-linked 99, syndromic, female-restricted [MIM: 300968]).[19]

Herein, we report ten unrelated individuals exhibiting a syndromic form of intellectual disability (ID) due to copy-number variant (CNV) deletions or single-nucleotide variants (SNVs) involving *PSMD12* (MIM: 604450), encoding the 456-amino-acid non-ATPase subunit PSMD12 (or RPN5) of the 26S proteasome. The compilation of this case series resulted from an international collaborative effort among Western France consortium HUGODIMS (Hôpitaux Universitaires du Grand Ouest pour l'Exploration par Approche Exome des Causes Moléculaires de Déficience Intellectuelle Isolée ou Syndromique Modérée à Sévère), Baylor Genetics Laboratories (BG), Boston Children's Hospital and GeneDX, the Simons Simplex Collection, Centre Hospitalier Universitaire (CHU) de La Réunion and Hôpital Robert Debré, and CHU de Toulouse. It was also partly facilitated by the web-based tools GeneMatcher[20] and DECIPHER.[21]

This study was approved by both the CHU de Nantes ethics committee (comité consultatif sur le traitement de l'information en matière de recherche no. 14.556) and the Baylor College of Medicine institutional review board. All participants were clinically assessed by at least one expert clinical geneticist from one of the participating centers. Written informed consent was obtained from all study participants. The main clinical features of our cohort are summarized in Table 1. More detailed clinical information for all subjects is provided in the Supplemental Note and Table S1, and corresponding Human Phenotype Ontology terms are reported in Tables S2 and S3.

Three de novo nonsense SNVs in *PSMD12* (GenBank: NM_002816.3)—c.367C>T (p.Arg123*) in subject 1, c.1274T>G (p.Leu425*) in subject 2, and c.601C>T (p.Arg201*) in subject 3—were found by subject-parent trio-based whole-exome sequencing. The protocols used

by each participating center have been detailed elsewhere.[22–24] These three variants were confirmed by Sanger sequencing. They were unique events observed in our in-house database of about 350 exomes (including 75 trios from families with simplex ID) for subject 1 (HUGODIMS and CHU de Nantes); in over 40,000 exomes, including 2,300 trios with various developmental disorders, for subject 2 (Boston Children's Hospital and GeneDX); and in 2,500 trios with autism spectrum disorders for subject 3 (Simons Simplex Collection) (Figure S2). These three variants are also absent in public variant databases (dbSNP138, 1000 Genomes, NHLBI GO Exome Sequencing Project, and the Exome Aggregation Consortium [ExAC] Browser). In addition, a query of over 7,000 clinical exomes in the BG database, according to the previously defined clinical diagnostics protocol,[25,26] revealed de novo splicing variant c.909−2A>G (p.?) in subject 4 (Figure S2). Differently sized de novo CNV deletions on 17q24.2 were found in four unrelated individuals (subjects 5, 6, 9, and 10) among 59,092 subjects referred for chromosomal microarray analysis (CMA) at BG between January 4, 2004, and May 6, 2016; they were tested with customized exon-targeted oligonucleotide arrays (OLIGO V8, V9, and V10) designed at BG,[27,28] which cover more than 4,800 known or candidate disease genes with exon-level resolution. The two remaining individuals, subjects 7 and 8, were recruited via DECIPHER (accession numbers 286468 and 300694). The largest CNV deletion in the series is about 4 Mb in size and includes *PSMD12* and 27 other genes, whereas the smallest deletion, 0.62 Mb, encompasses *PSMD12*, *PITPNC1* (MIM: 605134), and a portion of *HELZ* (MIM: 606699) (Figure 1 and Table S4). Minimal and maximal coordinates of the CNV deletions are indicated in Tables 1 and S1. In the BG in-house database, apparently similarly sized ~270 kb 17q24.2 duplication CNVs (chr17: 65,081,882–65,388,883 and 65,120,043–65,458,702; UCSC Genome Browser hg19), involving the entire *PSMD12*, were observed in three unrelated families. In two of these families, the duplication was inherited from the reportedly asymptomatic parents. Moreover, in one of these families, a pathogenic de novo CNV deletion in chromosomal region 2p14p15, explaining the subject's phenotype, was detected. Thus, this duplication most likely represents a rare nonpathogenic CNV. No constitutive de novo small duplication was recorded in DECIPHER[21] or in the Database of Genomic Variants.[29]

All subjects from the case series exhibited developmental delay (DD) or ID (n = 10) and had variable dysmorphic features, among which low-set ears (n = 6), hypertelorism (n = 5), and retrognathia or microretrognathia (n = 4) were the most frequent. All but one individual had additional neurological features, including abnormal behavior (n = 7, mostly autistic features or hyperactivity), hypotonia (n = 6), or epilepsy (n = 3, including seizure disorder, reflex seizures, and tonic convulsion). Additionally, two of six subjects had abnormalities detected on brain imaging (pineal cyst [n = 2], cerebral atrophy, and periventricular hypomyelination [n = 1]). Nine subjects had other congenital anomalies, including an atrio- or ventriculoseptal defect, patent ductus arteriosus, a single or dysplastic kidney, hydronephrosis, or genital anomalies (hypospadias or cryptorchidism). Five subjects had a history of feeding difficulties evident already in the neonatal period and associated with growth failure in four cases. Three subjects required gastrostomy feeding tubes. Seven subjects also had ophthalmologic anomalies, including strabismus, vision loss, and coloboma. Five subjects had skeletal abnormalities, including bilateral syndactyly of the second and third toes (n = 3) and thumb agenesis or hypoplasia (n = 2). Microcephaly was noted in five subjects, whereas macrocephaly was noted in one subject.

The 26S proteasome is a high-molecular-weight multisubunit proteinase complex of nearly 2.5 MDa whose structure, assembly, and functions are highly conserved across eukaryotes[1,5,30] (Figure S3). It is composed of two functionally distinct subcomplexes and responsible for the ATP-dependent degradation of poly-ubiquitinated proteins. The 19S regulatory particle (~900 kDa) binds and unfolds the ubiquitinated substrates, and the 20S proteolytic core (~700 kDa) is responsible for the hydrolysis of the substrate proteins.[31,32] The 19S particle, attached at either or both ends of the 20S particle, consists of two sub-complexes, the base and the lid. The base is composed of six ATPases (regulatory particle triple A proteins RPT1–RPT6), two large organizing subunits (regulatory particle non-ATPases 1 [RPN1] and 2 [RPN2]), and two ubiquitin receptors (RPN10 and RPN13).[1,31–34] The lid is formed from the deubiquitylating enzyme RPN11 and eight non-ATPase subunits (RPN3, RPN5–RPN9, RPN12, and RPN15), containing the PCI (proteasome-CSN [COP9 signalosome]-eIF3 [eukaryotic translation initiation factor 3]) domains.[1,31–34] Whereas the base acts as a reverse chaperone, unfolding and translocating substrate proteins into the 20S cavity, the lid ensures substrate recognition, deubiquitination, and scaffolding.[1,31,32,35,36]

All variants reported in the present case series involve *PSMD12*, which encodes PSMD12 (aka RPN5), one of the nine subunits of the 19S lid. We therefore speculated that the above functions of the 19S lid, and thereby those of the 26S proteasome, would be substantially altered in the described subjects. Experiments in fission yeast have stressed the importance of PSMD12 dosage in the regulation of proteasome 26S assembly and the maintenance of its structural integrity.[36] Moreover, in budding yeast, PSMD12 can stabilize both the proteasome and CSN.[33,37,38]

The most likely pathogenic dysfunction for the presented disorder is *PSMD12* haploinsufficiency. *PSMD12* has a very high haploinsufficiency score (HI index = 5.57%; HI index represents the predicted probability that a gene will exhibit haploinsufficiency in comparison to a large set of genes tested by DECIPHER: high-ranked genes [e.g., HI 0%–10%] are more likely to exhibit haploinsufficiency than low-ranked ones [e.g., 90%–100%]).[39] *PSMD12* is also predicted to be highly intolerant to loss-of-function (LoF)

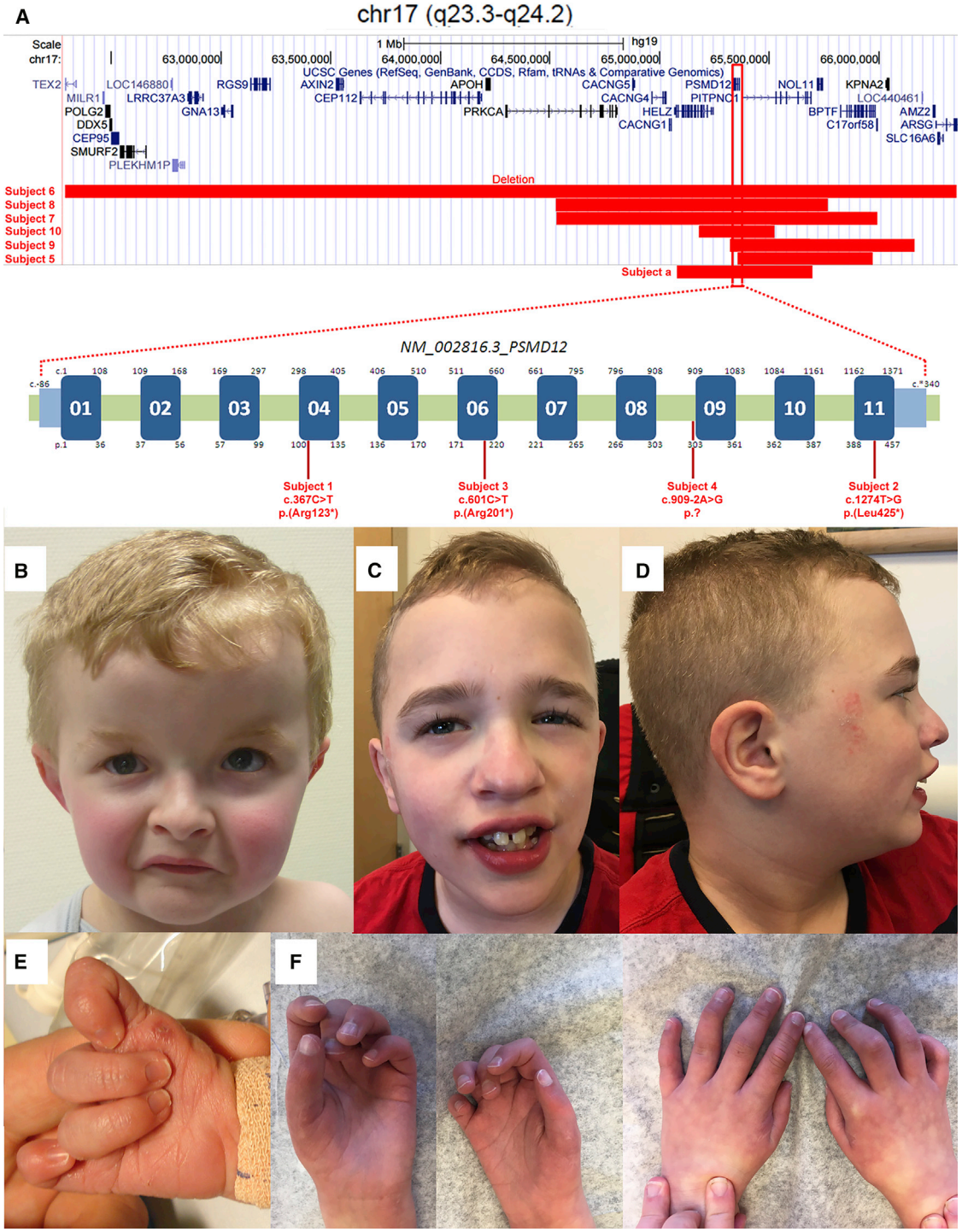

Figure 1. Mapping and Localization of the Ten *PSMD12* Variants and Morphological Anomalies in Subjects 1 and 2
A schematic representation of chromosomal region 17q24.2 shows the breakpoints of the CNV deletions encompassing *PSMD12* and localizations of the SNVs within the gene (A). Facial and hand anomalies are shown for subjects 1 (B and E) and 2 (C, D, and F). Consent for the publication of photographs was obtained for the two subjects. One additional subject with a neurodevelopmental disorder (subject a) with a smaller deletion involving *PSMD12* was tested by our CMA, albeit the detailed descriptions cannot be provided here because of privacy concerns.

mutations (probability of LoF intolerance = 1.00 with 1 observed LoF variant versus 21.5 predicted, according to the ExAC Browser).[40] Furthermore, we observed only heterozygous truncating variants or whole-gene deletions in the presented subjects. The only LoF variant reported in the ExAC Browser is predicted to alter the splicing of an in-frame *PSMD12* exon outside the functional domains of PSMD12; thus, LoF of this variant remains uncertain.

Given that the mutation c.1274T>G (p.Leu425*) in subject 2 is located in the last exon of *PSMD12*, it is predicted

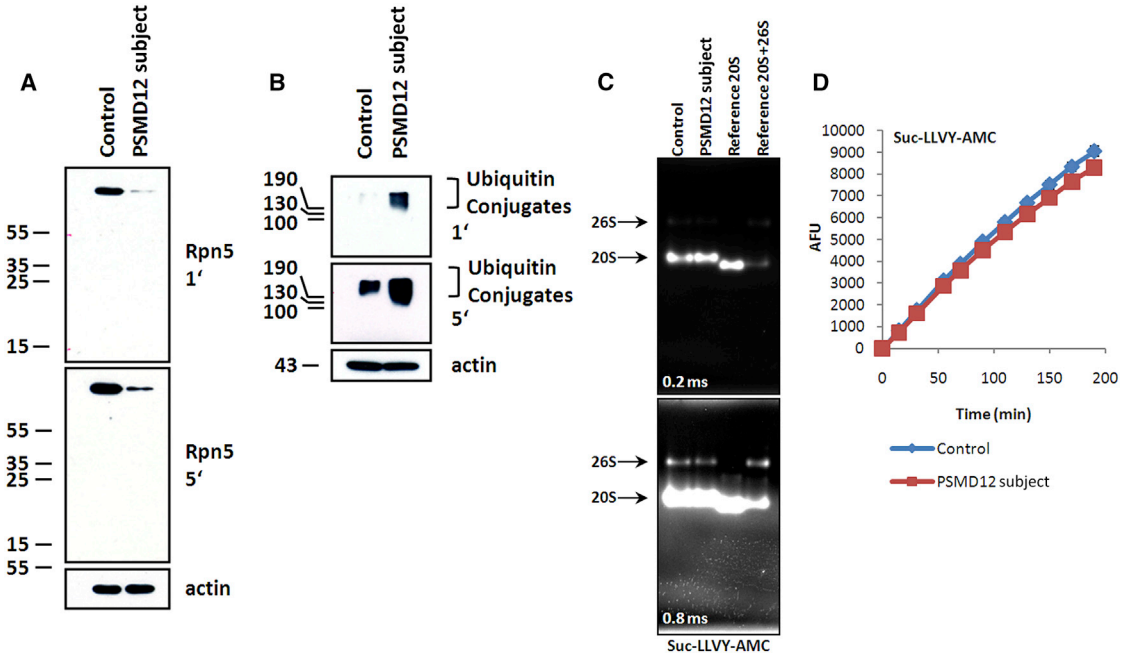

Figure 2. The c.367C>T (p.Arg123*) *PSMD12* Nonsense Mutation Leads to Decreased Levels of the Full-Length PSMD12 and Increased Accumulation of High-Molecular-Weight Ubiquitin-Modified Proteins without Altering the 20S or 26S Proteasome Complex

(A) PSMD12 (RPN5) content was determined with the H-3 monoclonal antibody (Santa Cruz Biotechnology) by western blotting. Protein extracts were prepared (as previously described[44]) from PBMCs from a healthy donor (control) and subject 1, who harbors the c.367C>T (p.Arg123*) *PSMD12* nonsense mutation. 10 μg were resolved by SDS-PAGE prior to western blotting with antibodies specific to PSMD12. For ensuring equal protein loading, the membrane was probed with a monoclonal antibody specific to β-actin (clone C4, Santa Cruz Biotechnology). Two exposure times, 1 min (above) and 2 min (below), are shown.

(B) Analysis of ubiquitin-protein conjugates in PBMCs derived from healthy (control) donors and subject 1, who harbors the c.367C>T (p.Arg123*) *PSMD12* nonsense mutation. Proteins were separated on 15% SDS gel in the presence of β-mercaptoethanol. The concentration of ubiquitin-modified proteins was determined by western blotting using an anti-ubiquitin antibody (reference no. Z0458, DAKO GmbH). For confirming equal protein loading in each lane, the membrane was probed with anti-β-actin antibody.

(C) Cell extracts from PBMCs derived from control subjects and subject 1 (who harbors the c.367C>T [p.Arg123*] nonsense mutation) were prepared with a detergent-free lysis buffer (TSDG) as previously described.[45,46] 20 μg of extract was subsequently exposed to 0.2 mM of the Suc-LLVY-AMC substrate (Bachem) and analyzed on 3%–12% gradient gels (native PAGE, Invitrogen) for chymotrypsin-like activity. Size controls consisted of 1 μg of purified spleen-derived 20S and/or 26S complex, as indicated. A gel-overlay assay for peptidase activity revealed two strongly staining bands corresponding to the 20S (670 kDa) and 26S (2 MDa) proteasome complexes in these cells. Of note, compared with the 20S reference, the 20S complex ran a little bit longer than the expected size, as evidenced by the upward shift in migration on the gel. The increased size of the 20S proteasome complex in these cells could be attributed to its association with additional interacting partners, such as PA28, which is constitutively present in immune cells.[45] Two acquisition times, 0.2 ms (above) and 0.8 ms (below), are shown.

(D) 10 μg of whole-cell lysate from PBMCs prepared from control subjects and subject 1 with TSDG buffer were incubated in a final 100 μL volume containing 0.2 mM Suc-LLVY-AMC in quadruplicate and in the presence of 2 mM ATP/DTT for various periods of time, as indicated. To determine the AMC cleavage rate reflecting the chymotrypsin-like activity, we monitored the fluorescence by using a plate reader at an excitation wavelength of 360 nm and emission wavelength of 460 nm during a period of 180 min.

to escape nonsense-mediated mRNA decay (NMD) and disrupt the PCI domain, which is essential for scaffolding involved in protein-protein interactions among the proteasome, CSN, and eIF3[41] (Figure S4). Notably, PSMD12 is integrated in the CSN and proteasome through its C-terminal portion of the PCI domain.[42] Thus, the truncated PSMD12 might fail to integrate properly with the proteasome lid.[43]

We sought to determine the functional consequences of the p.Arg123* nonsense variant in peripheral-blood mononuclear cells (PBMCs) collected from subject 1. We observed that the steady-state level of the full-length PSMD12 was significantly lower in subject 1's PBMC lysates than in those of a healthy donor (Figure 2A). The observation that the functional loss of one copy of *PSMD12* cannot be further compensated indicates that this gene is haploinsufficient, which is in line with the bioinformatic predictions and with the dramatic effect on embryogenesis associated with Psmd12 (Rpn5)-truncating variants in *Arabidopsis thaliana*.[35] Importantly, western blot analyses in subject 1's blood samples did not reveal the presence of the 122-amino-acid truncated protein with a predicted molecular mass of 13.796 kDa emerging from the *PSMD12* mutated allele. According to the manufacturer, the anti-PSMD12 antibody was raised against the first 300 amino acids of PSMD12, although the precise epitope sequence is not known. Therefore, one possible explanation for our failure to detect the truncated $PSMD12_{1–122}$ could be that the epitope recognized by the antibody is located downstream of the first 122 amino

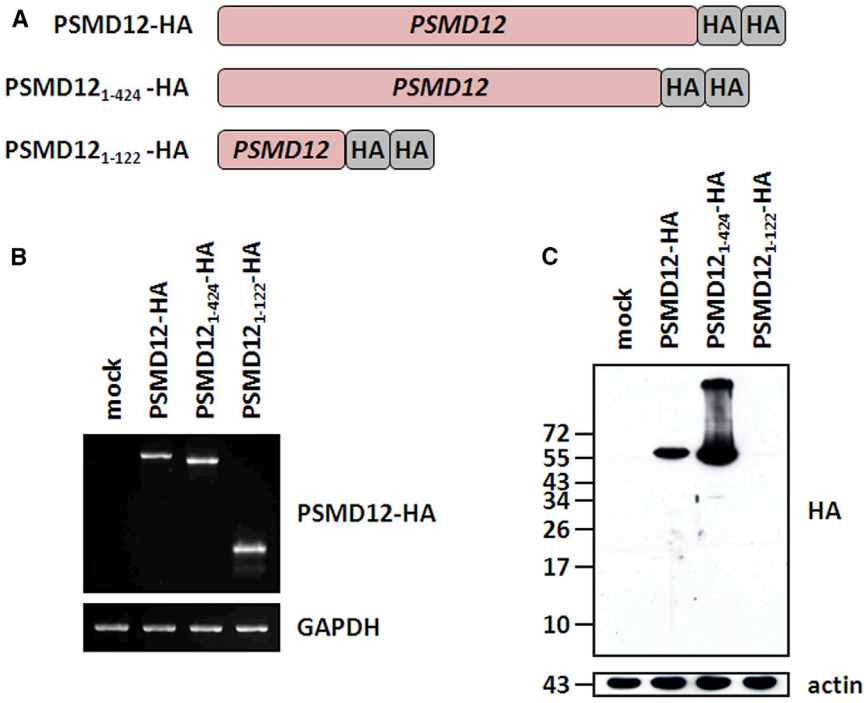

Figure 3. The c.367C>T *PSMD12* Mutant Is Efficiently Transcribed but Fails to Generate a Truncated Mature PSMD12$_{1–122}$

(A) Depiction of the PSMD12 constructs used in this study. The truncated PSMD12$_{1–424}$ and PSMD12$_{1–122}$ variants were constructed to reflect the Leu425* and Arg123* nonsense mutants, respectively. All PSMD12 constructs were cloned into the pcDNA3.1/Zeo(+) expression vector (Invitrogen) and C-terminally tagged with a double human influenza hemagglutinin (HA) epitope (GYPYDVPDYAMGGY PYDVPYAGT), as indicated.

(B) HeLa cells were cultivated in RPMI medium supplemented with 10% fetal calf serum and 1% penicillin and streptomycin (all purchased from Biochrom AG) and transfected with each of the three PSMD12 variants for 24 hr with Lipofectamin 2000 according to the manufacturer's instructions. Total RNA was extracted and analyzed by RT-PCR with forward and reverse primers specific to PSMD12 and HA, respectively. Equal loading in each lane was ensured by the amplification of GAPDH.

(C) HeLa cells transfected with the empty vector (mock) or each of our PSMD12 variants were subjected to protein extraction at 24 hr after transfection. Whole-cell extracts (20 μg) were resolved on 15% SDS-PAGE and subsequently analyzed by western blotting using anti-HA (clone 16B12, BioLegend) and anti-β-actin (loading control) antibodies, as indicated.

acids of PSMD12. Alternatively, it is also conceivable that our inability to detect the predicted PSMD12$_{1–122}$ short variant might be due to NMD and/or particular high proteolytic sensitivity and subsequent instability. To answer this question, we engineered tumor cells to produce hemagglutinin-tagged versions of both the wild-type PSMD12 and the truncated PSMD12$_{1–122}$ and PSMD12$_{1–424}$ variants emerging from the c.367T>C (p.Arg123*) and c.1274T>G (p.Leu425*) nonsense mutations, respectively (Figure 3A). As illustrated in Figures 3B and 3C, although all three constructs exhibited comparable levels of mRNA transcripts, protein levels were detected only for the wild-type and PSMD12$_{1–424}$ variant. This unambiguously indicates that our inability to detect the PSMD12$_{1–122}$ short variant was not due to NMD but rather reflects translation inefficiency and/or an increased degradation rate. Our in vitro data also show that the p.Arg123* nonsense mutant was accompanied by an increased accumulation of the high-molecular-weight ubiquitin-modified proteins (Figure 2B). This finding is consistent with the accumulation of polyubiquitinated proteins reported in yeasts with heterozygous loss of Rpn5,[36] indicating a role for PSMD12 in the maintenance of ubiquitin homeostasis. Importantly, the capacity of 26S complexes to degrade the Suc-LLVY (succinyl-Leu-Leu-Val-Tyr-amido-4-methylcoumarine) model substrate was not statistically different between the affected and control subjects (Figures 2C and 2D), indicating that both of these samples exhibit similar chymotrypsin-like activities. This finding further suggests that the elevated levels of such ubiquitin-protein conjugates in affected subjects did not result from a lower chymotrypsin activity of proteasomes. Rather, the decreased amount of PSMD12 might drive a conformational change of the 19S regulatory particle to render it deficient. In particular, PSMD12 is positioned in close proximity to the PSMD14 (RPN11) subunit,[47] which is involved in the hydrolysis of ubiquitin chains from targeted substrates before degradation by the 26S proteasome.[48] As such, the activity of PSMD14 might be affected in subjects with a downregulation of PSMD12, thereby resulting in impaired breakdown of ubiquitin-protein conjugates, which would mechanically increase the levels of polyubiquitinated substrate proteins. Alternatively, the increased accumulation of ubiquitin-modified proteins in subject 1, who carries the p.Arg123* nonsense variant, might also reflect a decreased accessibility of these substrates to the 26S proteasome through decreased amounts of incorporated RPN10 and RPN13.

Because the individuals with the *PSMD12* nonsense variants presented with central nervous system, renal, and craniofacial pathologies, we next sought to determine the function of PSMD12 during brain, kidney, and craniofacial development by utilizing the zebrafish embryo as an in vivo model. Considering the presence of disrupting mutations, we decided to use CRISPR/Cas9 technology to generate a mutant for the zebrafish ortholog of *PSMD12*. Using reciprocal BLAST, we identified a single zebrafish *PSMD12* ortholog (GenBank: NM_201578 and NP_963872) with 86% similarity and designed short guide RNA (sgRNA) targeting exon 3 of *psmd12* (Figure S5).

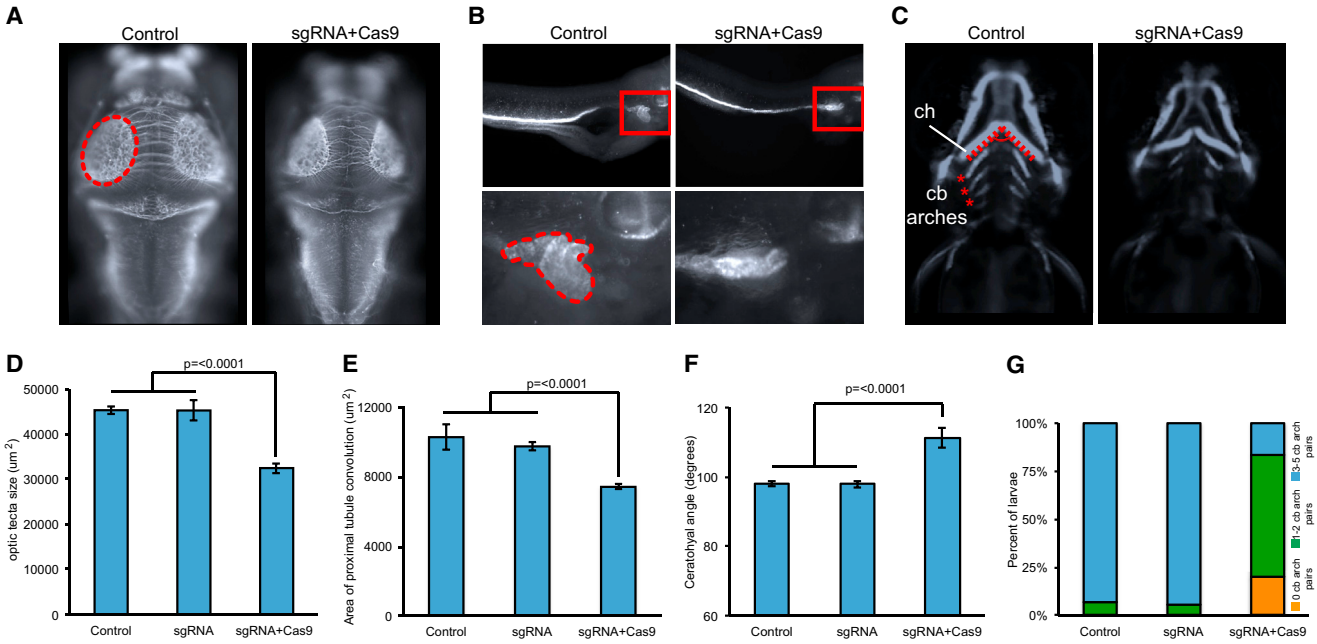

Figure 4. *psmd12* CRISPR/Cas9 Mutants Exhibit Microcephaly, Renal Tubular Atrophy, and Aberrant Rostrocaudal Patterning of the Branchial Arches in Zebrafish Larvae

(A) Representative dorsal images of 3 dpf zebrafish larvae stained with anti-acetylated tubulin show a reduction of the optic tecta (dotted oval) in F0 mutants.

(B) Representative lateral images of 4-day-old zebrafish larvae stained with anti-Na^+/K^+ ATPase alpha-1 subunit show a reduction in the convolution of the pronephric tubule (zoomed in and bordered with dotted shape in the lower panel) in F0 mutants.

(C) Representative ventral views of *-1.4col1a1:egfp* F0 mutant larvae imaged live at 3 dpf show an increase in the ceratohyal angle (ch, dotted line) and a reduction in pairs of bronchial arches (asterisks) in F0 mutants. cb, ceratobranchial.

(D) Size quantification of the optic tecta in F0 mutants targeted with CRISPR sgRNA ($p \leq 0.0001$ versus control, n = 30–50 larvae/batch, repeated).

(E) Quantification of the area of pronephric tubule convolution in F0 mutants targeted with sgRNA ($p \leq 0.0001$, n = 30–47 larvae/batch, repeated).

(F) Quantification of the ceratohyal angle in F0 mutants targeted with sgRNA ($p \leq 0.0001$, n = 32–44 larvae/batch, repeated).

(G) Categorization of F0 mutants based on pairs of ceratobranchial arches (n = 32–44 larvae/batch, repeated and observed with similar results).

Error bars represent the SEM.

CRISPR guide RNA was designed with ChopChop software (see guide sequences in Table S6) and synthesized with the GeneArt Precision gRNA Synthesis Kit (Invitrogen) according to the manufacturer's instructions. In brief, we mixed the forward and reverse target oligonucleotides, the Tracr fragment, and T7 primer mix with 2× Phusion High-Fidelity PCR Master Mix (Invitrogen) and then amplified and ran them on a 1% agarose gel to ensure the quality and appropriate size of the resulting CRISPR guide DNA template. We synthesized guide RNA by in vitro transcription with the TranscriptAid Enzyme Mix (Invitrogen) by incubating it at 37°C for 2 hr. After treatment with DNase I, the guide RNA was purified with the GeneArt gRNA Clean-Up Kit (Invitrogen). For CRISPR/Cas9-based genome editing, 100 pg of CRISPR guide RNA and 200 pg of Cas9 (GeneArt Platinum Cas9 Nuclease, Invitrogen) were injected into 1-cell-stage zebrafish embryos. The CRISPR/Cas9 efficiency was assessed as previously described.[49] In brief, DNA from each 2 day post fertilization (dpf) F0 embryo was extracted by proteinase K digestion (Life technologies, AM2548). The CRISPR-targeted region was amplified by PCR. We then denatured and slowly reannealed the PCR products to facilitate the formation of heteroduplexes (denaturing at 95°C for 5 min, ramped down to 85°C at −1°C/s and then to 25°C at −0.1°C/s). Heteroduplexes were detected on 15% polyacrylamide gel electrophoresis 23 (n = 6 F0 embryos tested/condition). Then, we cloned and sequenced PCR amplicons to estimate the mosaicism. Ultimately, we observed ≈90% mosaicism.

Given the presence of microcephaly in most of our subjects, we next measured the size of the optic tecta as a readout for head size[50] of the F0 *psmd12* zebrafish mutants. Standard whole-mount zebrafish immunostaining was performed on CRISPR experiments as previously described.[49,50] To visualize the axonal tracts in the brain, including the optic tecta and the cerebellum, we stained 3 dpf mutant and control embryos with an anti-acetylated tubulin primary antibody (T7451, mouse, Sigma-Aldrich; 1:1,000 dilution) and the Alexa Fluor goat anti-mouse IgG (A21207, Invitrogen; 1:500 dilution) as a secondary antibody.[50] We observed that the size of the optic tecta was significantly smaller in CRISPR F0 mutants than in the control larvae ($p \leq 0.0001$, n = 30–50 larvae/batch, repeated; Figures 4A and 4D).

In addition, we assessed whether *psmd12* was also required for renal development by quantifying the area of proximal tubule convolution in 4 dpf F0 *psmd12* mutants stained with an anti-Na^+/K+ ATPase alpha-1 subunit primary antibody (α6F, DSHB; 1:20 dilution) and Alexa Fluor rabbit anti-mouse IgG secondary antibody (Invitrogen; 1:500 dilution). Compared to controls, which showed properly convoluted tubules, mutant zebrafish embryos displayed qualitative defects of the proximal tubule, including absent, reduced, or v-shaped tubules. Using ImageJ software, we then measured the area of the renal tubules in both mutants and controls and observed that the area of the proximal convolution was significantly smaller in F0 mutants ($p \leq 0.0001$, n = 30–47 larvae/batch, repeated) than in controls (Figures 4B and 4E). We did not observe any larvae with a unilateral or bilateral absence of kidneys.

It has been previously shown that zebrafish models of mispatterned craniofacial cartilage reflect craniofacial abnormalities in humans.[51–53] Finally, to assess the role of *psmd12* in craniofacial development, we therefore injected CRISPR sgRNA into the *-1.4col1a1:egfp* transgenic line embryos at the 1-cell stage. *-1.4col1a1:egfp* demonstrates GFP signal in cartilages. This transgenic line contains a 1.4 kb proximal promoter fragment of Col1a1 inserted upstream of Egfp.[54] For imaging, 3 dpf larvae were positioned and imaged live with the Vertebrate Automated Screening Technology platform (version 1.2.2.8, Union Biometrica) in a manner similar to previously described methods.[53,55] We assessed craniofacial patterning by either measuring the angle of the ceratohyal cartilage at 3 dpf or by counting the number of ceratobranchial arch pairs at 3 dpf. We were then able to quantify two types of craniofacial abnormalities from GFP-positive cells in *-1.4col1a1:egfp* CRISPR F0 mutants. First, we observed a significantly broadened angle of the ceratohyal in F0 mutants ($p \leq 0.0001$, n = 32–44 larvae/batch, repeated; Figures 4C and 4F). Second, we observed a significant delay in rostrocaudal ceratobranchial (cb) arch patterning; F0 mutants showed a reduced number of cb pairs (Figures 4C and 4G).

Taken together, our data indicate that *PSMD12* plays an important role during brain, kidney, and craniofacial development and that its LoF leads to defects that are reminiscent of the phenotypes observed in our subject cohort.

The high expression of *PSMD12* in the frontal cortex (Figures S6–S8) is consistent with the main neurological component in the neurodevelopmental syndrome presented here. In support of this notion, CNV deletions of *PSMD12* were reported in two independent investigations on subjects with ID, truncal obesity, and psychiatric symptoms.[56,57] In the first study, three subjects with a complete deletion of *PSMD12* had conductive hearing loss and feeding difficulties during infancy in addition to ID.[57] In the second study, the subject with a large deletion including *PSMD12* exhibited global DD associated with a cardiac defect, feeding difficulties, and pulmonary infection,[56] clinical findings consistent with those reported in our study.

Thus far, two other genes encoding subunits of the proteasome 26S have been proposed to be associated with syndromic ID. The first gene, *PSMD14* (MIM: 607173), encodes the deubiquitinating enzyme PSMD14 (RPN11)[47,58] and was included in the 2q24.2 deletion harboring two other genes: *TBR1* (MIM: 604616), whose LoF mutations are associated with autism,[59] and *TANK* (MIM: 604834), identified in an individual with ID and short stature.[60] In a subject with a balanced complex chromosomal aberration (reciprocal translocation and paracentric inversion), *PSMD14* was considered a strong neurodevelopmental candidate gene.[61] As mentioned above, PSMD12 would need to directly interact with PSMD14 to acquire its active enzymatic conformation.[47,62] The second gene, *PSMA7*, encodes an alpha subunit of the 20S core complex. A de novo heterozygous likely pathogenic variant was found in a subject with severe ID, premature baldness, retrognathia, mild kyphosis, hirsutism, and short toes.[63]

Interestingly, PSMD12 is predicted to have direct interactions with other proteins of the UPS signaling pathway: UBE3A, UBE3B, HUWE1, USP7, and USP9X, whose dysfunction is associated with ID (Figure S9).

In conclusion, we describe a neurodevelopmental disorder caused by de novo heterozygous inactivating point mutations or CNV deletions of *PSMD12*. Future studies will attempt to unravel the impact of PSMD12 downregulation on the incorporation efficiency of other subunits into the 19S regulatory particle. These investigations would represent initial steps toward determining how proteome remodeling caused by LoF *PSMD12* variants can lead to ID, congenital malformations, and other clinical features of this neurodevelopmental syndrome.

Accession Numbers

PSMD12 sequence variants c.367C>T (p.Arg123*), c.1274T>G (p.Leu425*), c.601C>T (p.Arg201*), and c.909−2A>G (p.?) have been deposited in the Leiden Open Variation Database under accession numbers LOVD: 0000132255, 0000132256, 0000132257, and 0000132258, respectively.

Supplemental Data

Supplemental Data include a Supplemental Note, ten figures, and six tables and can be found with this article online at http://dx.doi.org/10.1016/j.ajhg.2017.01.003.

Acknowledgments

We would like to thank all families for participating in this study. We acknowledge HUGODIMS (a Western France exome-based trio-approach project to identify genes involved in intellectual disability); funding for HUGODIMS (subject 1) is supported by a grant from the French Ministry of Health and from the Health Regional Agency from Poitou-Charentes (HUGODIMS, 2013, RC14_0107). We thank Dr. Frédérique Allaire from the Health Regional Agency of Poitou-Charentes for supporting this project. We thank Léa Ferrand and Emilie Le Blanc for grant and data management. We acknowledge GEM HUGO (Western France Network

of Medical Genetics and Genomics). We are most grateful to the Nantes Genomics core facility (Biogenouest Genomics) for its technical support and for performing exome sequencing for subject 1 and his parents. This work was supported in part by grant U54HG006542 from the US National Human Genome Research Institute and National Heart, Lung, and Blood Institute to the Baylor Hopkins Center for Mendelian Genomics. This study made use of data generated by the DECIPHER community. A full list of centers who contributed to data generation is available at http://decipher.sanger.ac.uk and via email at decipher@sanger.ac.uk. Funding for the project was provided by the Wellcome Trust. M.T.C, K.G.M, and K.R. are employees of GeneDx.

Received: November 3, 2016
Accepted: January 4, 2017
Published: January 26, 2017

Web Resources

1000 Genomes, http://www.1000genomes.org/
ChopChop software, https://chopchop.rc.fas.harvard.edu/
Database of Genomic Variants, http://dgv.tcag.ca/dgv/app/home/
DECIPHER, https://decipher.sanger.ac.uk/
dbSNP, http://www.ncbi.nlm.nih.gov/projects/SNP/
GeneMatcher, https://genematcher.org/
ExAC Browser, http://exac.broadinstitute.org/
GenBank, http://www.ncbi.nlm.nih.gov/genbank/
Leiden Open Variation Database, http://www.lovd.nl/
NHLBI Exome Sequencing Project (ESP) Exome Variant Server, http://evs.gs.washington.edu/EVS/
OMIM, http://www.omim.org/
PLINK, http://pngu.mgh.harvard.edu/~purcell/plink/
The Human Protein Atlas, http://www.proteinatlas.org/
UCSC Genome Browser, http://genome.ucsc.edu

References

1. Sullivan, J.A., Shirasu, K., and Deng, X.W. (2003). The diverse roles of ubiquitin and the 26S proteasome in the life of plants. Nat. Rev. Genet. *4*, 948–958.
2. Goldberg, A.L. (2003). Protein degradation and protection against misfolded or damaged proteins. Nature *426*, 895–899.
3. Hershko, A., and Ciechanover, A. (1998). The ubiquitin system. Annu. Rev. Biochem. *67*, 425–479.
4. Finley, D. (2009). Recognition and processing of ubiquitin-protein conjugates by the proteasome. Annu. Rev. Biochem. *78*, 477–513.
5. Murata, S., Yashiroda, H., and Tanaka, K. (2009). Molecular mechanisms of proteasome assembly. Nat. Rev. Mol. Cell Biol. *10*, 104–115.
6. Voges, D., Zwickl, P., and Baumeister, W. (1999). The 26S proteasome: a molecular machine designed for controlled proteolysis. Annu. Rev. Biochem. *68*, 1015–1068.
7. Hamilton, A.M., and Zito, K. (2013). Breaking it down: the ubiquitin proteasome system in neuronal morphogenesis. Neural Plast. *2013*, 196848.
8. Tai, H.C., and Schuman, E.M. (2008). Ubiquitin, the proteasome and protein degradation in neuronal function and dysfunction. Nat. Rev. Neurosci. *9*, 826–838.
9. Cajigas, I.J., Will, T., and Schuman, E.M. (2010). Protein homeostasis and synaptic plasticity. EMBO J. *29*, 2746–2752.
10. Hegde, A.N., Haynes, K.A., Bach, S.V., and Beckelman, B.C. (2014). Local ubiquitin-proteasome-mediated proteolysis and long-term synaptic plasticity. Front. Mol. Neurosci. *7*, 96.
11. Acconcia, F., Sigismund, S., and Polo, S. (2009). Ubiquitin in trafficking: the network at work. Exp. Cell Res. *315*, 1610–1618.
12. Schwarz, L.A., and Patrick, G.N. (2012). Ubiquitin-dependent endocytosis, trafficking and turnover of neuronal membrane proteins. Mol. Cell. Neurosci. *49*, 387–393.
13. Dantuma, N.P., and Bott, L.C. (2014). The ubiquitin-proteasome system in neurodegenerative diseases: precipitating factor, yet part of the solution. Front. Mol. Neurosci. *7*, 70.
14. Fecto, F., Esengul, Y.T., and Siddique, T. (2014). Protein recycling pathways in neurodegenerative diseases. Alzheimers Res. Ther. *6*, 13.
15. Kishino, T., Lalande, M., and Wagstaff, J. (1997). UBE3A/E6-AP mutations cause Angelman syndrome. Nat. Genet. *15*, 70–73.
16. Basel-Vanagaite, L., Dallapiccola, B., Ramirez-Solis, R., Segref, A., Thiele, H., Edwards, A., Arends, M.J., Miró, X., White, J.K., Désir, J., et al. (2012). Deficiency for the ubiquitin ligase UBE3B in a blepharophimosis-ptosis-intellectual-disability syndrome. Am. J. Hum. Genet. *91*, 998–1010.
17. Froyen, G., Corbett, M., Vandewalle, J., Jarvela, I., Lawrence, O., Meldrum, C., Bauters, M., Govaerts, K., Vandeleur, L., Van Esch, H., et al. (2008). Submicroscopic duplications of the hydroxysteroid dehydrogenase HSD17B10 and the E3 ubiquitin ligase HUWE1 are associated with mental retardation. Am. J. Hum. Genet. *82*, 432–443.
18. Hao, Y.H., Fountain, M.D., Jr., Fon Tacer, K., Xia, F., Bi, W., Kang, S.H., Patel, A., Rosenfeld, J.A., Le Caignec, C., Isidor, B., et al. (2015). USP7 Acts as a Molecular Rheostat to Promote WASH-Dependent Endosomal Protein Recycling and Is Mutated in a Human Neurodevelopmental Disorder. Mol. Cell *59*, 956–969.
19. Homan, C.C., Kumar, R., Nguyen, L.S., Haan, E., Raymond, F.L., Abidi, F., Raynaud, M., Schwartz, C.E., Wood, S.A., Gecz, J., and Jolly, L.A. (2014). Mutations in USP9X are associated with X-linked intellectual disability and disrupt neuronal cell migration and growth. Am. J. Hum. Genet. *94*, 470–478.
20. Sobreira, N., Schiettecatte, F., Valle, D., and Hamosh, A. (2015). GeneMatcher: a matching tool for connecting investigators with an interest in the same gene. Hum. Mutat. *36*, 928–930.
21. Firth, H.V., Richards, S.M., Bevan, A.P., Clayton, S., Corpas, M., Rajan, D., Van Vooren, S., Moreau, Y., Pettett, R.M., and Carter, N.P. (2009). DECIPHER: Database of Chromosomal Imbalance and Phenotype in Humans Using Ensembl Resources. Am. J. Hum. Genet. *84*, 524–533.
22. Isidor, B., Küry, S., Rosenfeld, J.A., Besnard, T., Schmitt, S., Joss, S., Davies, S.J., Lebel, R.R., Henderson, A., Schaaf, C.P., et al. (2016). De Novo Truncating Mutations in the Kinetochore-Microtubules Attachment Gene CHAMP1 Cause Syndromic Intellectual Disability. Hum. Mutat. *37*, 354–358.
23. Retterer, K., Juusola, J., Cho, M.T., Vitazka, P., Millan, F., Gibellini, F., Vertino-Bell, A., Smaoui, N., Neidich, J., Monaghan, K.G., et al. (2016). Clinical application of whole-exome sequencing across clinical indications. Genet. Med. *18*, 696–704.
24. Iossifov, I., O'Roak, B.J., Sanders, S.J., Ronemus, M., Krumm, N., Levy, D., Stessman, H.A., Witherspoon, K.T., Vives, L., Patterson, K.E., et al. (2014). The contribution of de novo coding mutations to autism spectrum disorder. Nature *515*, 216–221.

25. Bainbridge, M.N., Wang, M., Wu, Y., Newsham, I., Muzny, D.M., Jefferies, J.L., Albert, T.J., Burgess, D.L., and Gibbs, R.A. (2011). Targeted enrichment beyond the consensus coding DNA sequence exome reveals exons with higher variant densities. Genome Biol. *12*, R68.
26. Yang, Y., Muzny, D.M., Reid, J.G., Bainbridge, M.N., Willis, A., Ward, P.A., Braxton, A., Beuten, J., Xia, F., Niu, Z., et al. (2013). Clinical whole-exome sequencing for the diagnosis of mendelian disorders. N. Engl. J. Med. *369*, 1502–1511.
27. Boone, P.M., Bacino, C.A., Shaw, C.A., Eng, P.A., Hixson, P.M., Pursley, A.N., Kang, S.H., Yang, Y., Wiszniewska, J., Nowakowska, B.A., et al. (2010). Detection of clinically relevant exonic copy-number changes by array CGH. Hum. Mutat. *31*, 1326–1342.
28. Wiszniewska, J., Bi, W., Shaw, C., Stankiewicz, P., Kang, S.H., Pursley, A.N., Lalani, S., Hixson, P., Gambin, T., Tsai, C.H., et al. (2014). Combined array CGH plus SNP genome analyses in a single assay for optimized clinical testing. Eur. J. Hum. Genet. *22*, 79–87.
29. MacDonald, J.R., Ziman, R., Yuen, R.K., Feuk, L., and Scherer, S.W. (2014). The Database of Genomic Variants: a curated collection of structural variation in the human genome. Nucleic Acids Res. *42*, D986–D992.
30. Gomes, A.V. (2013). Genetics of proteasome diseases. Scientifica (Cairo) *2013*, 637629.
31. Bhattacharyya, S., Yu, H., Mim, C., and Matouschek, A. (2014). Regulated protein turnover: snapshots of the proteasome in action. Nat. Rev. Mol. Cell Biol. *15*, 122–133.
32. Sharon, M., Taverner, T., Ambroggio, X.I., Deshaies, R.J., and Robinson, C.V. (2006). Structural organization of the 19S proteasome lid: insights from MS of intact complexes. PLoS Biol. *4*, e267.
33. Glickman, M.H., Rubin, D.M., Coux, O., Wefes, I., Pfeifer, G., Cjeka, Z., Baumeister, W., Fried, V.A., and Finley, D. (1998). A subcomplex of the proteasome regulatory particle required for ubiquitin-conjugate degradation and related to the COP9-signalosome and eIF3. Cell *94*, 615–623.
34. Rubin, D.M., Glickman, M.H., Larsen, C.N., Dhruvakumar, S., and Finley, D. (1998). Active site mutants in the six regulatory particle ATPases reveal multiple roles for ATP in the proteasome. EMBO J. *17*, 4909–4919.
35. Book, A.J., Smalle, J., Lee, K.H., Yang, P., Walker, J.M., Casper, S., Holmes, J.H., Russo, L.A., Buzzinotti, Z.W., Jenik, P.D., and Vierstra, R.D. (2009). The RPN5 subunit of the 26s proteasome is essential for gametogenesis, sporophyte development, and complex assembly in Arabidopsis. Plant Cell *21*, 460–478.
36. Yen, H.C., Espiritu, C., and Chang, E.C. (2003). Rpn5 is a conserved proteasome subunit and required for proper proteasome localization and assembly. J. Biol. Chem. *278*, 30669–30676.
37. Collins, S.R., Miller, K.M., Maas, N.L., Roguev, A., Fillingham, J., Chu, C.S., Schuldiner, M., Gebbia, M., Recht, J., Shales, M., et al. (2007). Functional dissection of protein complexes involved in yeast chromosome biology using a genetic interaction map. Nature *446*, 806–810.
38. Maytal-Kivity, V., Pick, E., Piran, R., Hofmann, K., and Glickman, M.H. (2003). The COP9 signalosome-like complex in S. cerevisiae and links to other PCI complexes. Int. J. Biochem. Cell Biol. *35*, 706–715.
39. Huang, N., Lee, I., Marcotte, E.M., and Hurles, M.E. (2010). Characterising and predicting haploinsufficiency in the human genome. PLoS Genet. *6*, e1001154.
40. Lek, M., Karczewski, K.J., Minikel, E.V., Samocha, K.E., Banks, E., Fennell, T., O'Donnell-Luria, A.H., Ware, J.S., Hill, A.J., Cummings, B.B., et al.; Exome Aggregation Consortium (2016). Analysis of protein-coding genetic variation in 60,706 humans. Nature *536*, 285–291.
41. Kim, H.M., Yu, Y., and Cheng, Y. (2011). Structure characterization of the 26S proteasome. Biochim. Biophys. Acta *1809*, 67–79.
42. Yu, Z., Kleifeld, O., Lande-Atir, A., Bsoul, M., Kleiman, M., Krutauz, D., Book, A., Vierstra, R.D., Hofmann, K., Reis, N., et al. (2011). Dual function of Rpn5 in two PCI complexes, the 26S proteasome and COP9 signalosome. Mol. Biol. Cell *22*, 911–920.
43. Peters, L.Z., Karmon, O., David-Kadoch, G., Hazan, R., Yu, T., Glickman, M.H., and Ben-Aroya, S. (2015). The protein quality control machinery regulates its misassembled proteasome subunits. PLoS Genet. *11*, e1005178.
44. Ebstein, F., Lehmann, A., and Kloetzel, P.M. (2012). The FAT10- and ubiquitin-dependent degradation machineries exhibit common and distinct requirements for MHC class I antigen presentation. Cell. Mol. Life Sci. *69*, 2443–2454.
45. Bochmann, I., Ebstein, F., Lehmann, A., Wohlschlaeger, J., Sixt, S.U., Kloetzel, P.M., and Dahlmann, B. (2014). T lymphocytes export proteasomes by way of microparticles: a possible mechanism for generation of extracellular proteasomes. J. Cell. Mol. Med. *18*, 59–68.
46. Seifert, U., Bialy, L.P., Ebstein, F., Bech-Otschir, D., Voigt, A., Schröter, F., Prozorovski, T., Lange, N., Steffen, J., Rieger, M., et al. (2010). Immunoproteasomes preserve protein homeostasis upon interferon-induced oxidative stress. Cell *142*, 613–624.
47. Dambacher, C.M., Worden, E.J., Herzik, M.A., Martin, A., and Lander, G.C. (2016). Atomic structure of the 26S proteasome lid reveals the mechanism of deubiquitinase inhibition. eLife *5*, e13027.
48. Boehringer, J., Riedinger, C., Paraskevopoulos, K., Johnson, E.O., Lowe, E.D., Khoudian, C., Smith, D., Noble, M.E., Gordon, C., and Endicott, J.A. (2012). Structural and functional characterization of Rpn12 identifies residues required for Rpn10 proteasome incorporation. Biochem. J. *448*, 55–65.
49. Bolar, N.A., Golzio, C., Živná, M., Hayot, G., Van Hemelrijk, C., Schepers, D., Vandeweyer, G., Hoischen, A., Huyghe, J.R., Raes, A., et al. (2016). Heterozygous Loss-of-Function SEC61A1 Mutations Cause Autosomal-Dominant Tubulo-Interstitial and Glomerulocystic Kidney Disease with Anemia. Am. J. Hum. Genet. *99*, 174–187.
50. Borck, G., Hög, F., Dentici, M.L., Tan, P.L., Sowada, N., Medeira, A., Gueneau, L., Thiele, H., Kousi, M., Lepri, F., et al. (2015). BRF1 mutations alter RNA polymerase III-dependent transcription and cause neurodevelopmental anomalies. Genome Res. *25*, 155–166.
51. Dauber, A., Golzio, C., Guenot, C., Jodelka, F.M., Kibaek, M., Kjaergaard, S., Leheup, B., Martinet, D., Nowaczyk, M.J., Rosenfeld, J.A., et al. (2013). SCRIB and PUF60 are primary drivers of the multisystemic phenotypes of the 8q24.3 copy-number variant. Am. J. Hum. Genet. *93*, 798–811.
52. Gordon, C.T., Weaver, K.N., Zechi-Ceide, R.M., Madsen, E.C., Tavares, A.L., Oufadem, M., Kurihara, Y., Adameyko, I., Picard, A., Breton, S., et al. (2015). Mutations in the endothelin receptor type A cause mandibulofacial dysostosis with alopecia. Am. J. Hum. Genet. *96*, 519–531.
53. Isrie, M., Breuss, M., Tian, G., Hansen, A.H., Cristofoli, F., Morandell, J., Kupchinsky, Z.A., Sifrim, A., Rodriguez-Rodriguez,

C.M., Dapena, E.P., et al. (2015). Mutations in Either TUBB or MAPRE2 Cause Circumferential Skin Creases Kunze Type. Am. J. Hum. Genet. *97*, 790–800.

54. Kague, E., Gallagher, M., Burke, S., Parsons, M., Franz-Odendaal, T., and Fisher, S. (2012). Skeletogenic fate of zebrafish cranial and trunk neural crest. PLoS ONE *7*, e47394.
55. Pardo-Martin, C., Allalou, A., Medina, J., Eimon, P.M., Wählby, C., and Fatih Yanik, M. (2013). High-throughput hyperdimensional vertebrate phenotyping. Nat. Commun. *4*, 1467.
56. Bartnik, M., Nowakowska, B., Derwińska, K., Wiśniowiecka-Kowalnik, B., Kędzior, M., Bernaciak, J., Ziemkiewicz, K., Gambin, T., Sykulski, M., Bezniakow, N., et al. (2014). Application of array comparative genomic hybridization in 256 patients with developmental delay or intellectual disability. J. Appl. Genet. *55*, 125–144.
57. Vergult, S., Dauber, A., Delle Chiaie, B., Van Oudenhove, E., Simon, M., Rihani, A., Loeys, B., Hirschhorn, J., Pfotenhauer, J., Phillips, J.A., 3rd., et al. (2012). 17q24.2 microdeletions: a new syndromal entity with intellectual disability, truncal obesity, mood swings and hallucinations. Eur. J. Hum. Genet. *20*, 534–539.
58. Cooper, E.M., Cutcliffe, C., Kristiansen, T.Z., Pandey, A., Pickart, C.M., and Cohen, R.E. (2009). K63-specific deubiquitination by two JAMM/MPN+ complexes: BRISC-associated Brcc36 and proteasomal Poh1. EMBO J. *28*, 621–631.
59. Notwell, J.H., Heavner, W.E., Darbandi, S.F., Katzman, S., McKenna, W.L., Ortiz-Londono, C.F., Tastad, D., Eckler, M.J., Rubenstein, J.L., McConnell, S.K., et al. (2016). TBR1 regulates autism risk genes in the developing neocortex. Genome Res. *26*, 1013–1022.
60. Burrage, L.C., Eble, T.N., Hixson, P.M., Roney, E.K., Cheung, S.W., and Franco, L.M. (2013). A mosaic 2q24.2 deletion narrows the critical region to a 0.4 Mb interval that includes TBR1, TANK, and PSMD14. Am. J. Med. Genet. A. *161A*, 841–844.
61. Blake, J., Riddell, A., Theiss, S., Gonzalez, A.P., Haase, B., Jauch, A., Janssen, J.W., Ibberson, D., Pavlinic, D., Moog, U., et al. (2014). Sequencing of a patient with balanced chromosome abnormalities and neurodevelopmental disease identifies disruption of multiple high risk loci by structural variation. PLoS ONE *9*, e90894.
62. Verma, R., Aravind, L., Oania, R., McDonald, W.H., Yates, J.R., 3rd, Koonin, E.V., and Deshaies, R.J. (2002). Role of Rpn11 metalloprotease in deubiquitination and degradation by the 26S proteasome. Science *298*, 611–615.
63. de Ligt, J., Willemsen, M.H., van Bon, B.W., Kleefstra, T., Yntema, H.G., Kroes, T., Vulto-van Silfhout, A.T., Koolen, D.A., de Vries, P., Gilissen, C., et al. (2012). Diagnostic exome sequencing in persons with severe intellectual disability. N. Engl. J. Med. *367*, 1921–1929.

The American Journal of Human Genetics, Volume *100*

Supplemental Data

De Novo Disruption of the Proteasome Regulatory Subunit *PSMD12* Causes a Syndromic Neurodevelopmental Disorder

Sébastien Küry, Thomas Besnard, Frédéric Ebstein, Tahir N. Khan, Tomasz Gambin, Jessica Douglas, Carlos A. Bacino, Stephan J. Sanders, Andrea Lehmann, Xénia Latypova, Kamal Khan, Mathilde Pacault, Stephanie Sacharow, Kimberly Glaser, Eric Bieth, Laurence Perrin-Sabourin, Marie-Line Jacquemont, Megan T. Cho, Elizabeth Roeder, Anne-Sophie Denommé-Pichon, Kristin G. Monaghan, Bo Yuan, Fan Xia, Sylvain Simon, Dominique Bonneau, Philippe Parent, Brigitte Gilbert-Dussardier, Sylvie Odent, Annick Toutain, Laurent Pasquier, Deborah Barbouth, Chad A. Shaw, Ankita Patel, Janice L. Smith, Weimin Bi, Sébastien Schmitt, Wallid Deb, Mathilde Nizon, Sandra Mercier, Marie Vincent, Caroline Rooryck, Valérie Malan, Ignacio Briceño, Alberto Gómez, Kimberly M. Nugent, James B. Gibson, Benjamin Cogné, James R. Lupski, Holly A.F. Stessman, Evan E. Eichler, Kyle Retterer, Yaping Yang, Richard Redon, Nicholas Katsanis, Jill A. Rosenfeld, Peter-Michael Kloetzel, Christelle Golzio, Stéphane Bézieau, Paweł Stankiewicz, and Bertrand Isidor

SUPPLEMENT (Table of contents)

SUPPLEMENTAL CASE REPORTS

Method of inclusion

The nine affected children selected in the present study were enrolled in six different programs or centers investigating the molecular basis of developmental disorders: the Western France consortium HUGODIMS (French acronym standing for "Projet inter-régional Français des Hôpitaux Universitaires du Grand Ouest pour l'exploration par approche exome des causes moléculaires de Déficience Intellectuelle isolée ou syndromique Modérée à Sévère"; Subject 1), the Boston Children's Hospital in collaboration with GeneDX laboratory (USA; Subject 2), the Simons Simplex Collection (Subject 3), the Baylor Genetics Laboratory (BG, Houston, TX, USA) clinical exome testing cohort (Subjects 4, 5, 6, 9 and 10), the University Hospital Centre of Toulouse (Purpan Hospital; Subject 7), and the University Hospital Centre of La Réunion/Robert Debré Hospital (Paris; Subject 8).

Clinical details

Subject 1 is the second child of non-consanguineous parents. The family history was unremarkable. The pregnancy was uncomplicated, with normal screening ultrasounds. He was delivered at term via vaginal delivery. At birth, he showed hypotonia and feeding difficulties, dysmorphic features including a large forehead, posterior plagiocephaly, dysplastic ears, and microretrognathia (Figure 1). Limbs examination showed right thumb agenesis and left thumb hypoplasia. Hypospadias was also noted. Cardiac ultrasound revealed a complex cardiopathy (atrial septal defect, ventricular septal defect, truncus arteriosus and aortic arch hypoplasia) which required surgery at one month. Gastrostomy was performed at two months of age.

In addition, he had bilateral profound sensorineural deafness, which was noted at the age of 10 months. He had an implant in his right ear at 3-year-old. CT-scan of the temporal bones showed normal cochlea and bilateral symmetrical vestibular abnormalities. The vestibules were dilated. There was a bilateral complete agenesis of the lateral semicircular canal and a rudimentary posterior semicircular canal. The olfactory bulbs were normal. Abdominal ultrasound showed kidneys fusion with a left pelvic kidney.

He was not able to sit independently until 14 months of age and to walk until 3 years and 6 months. At last evaluation, at the age of 8 years and 4 months, he still did not have any

recognizable speech. He still had severe feeding difficulties. He also showed recurrent pulmonary infections for which he has been hospitalized repeatedly.

Ophthalmological examination showed bilateral horizontal nystagmus and strabismus. MRI of the brain was considered as normal.

Using whole exome sequencing, a *de novo* PSMD12 mutation was identified: Chr17(Genome Reference Consortium human genome build (GRCh37)):g.65346383G>A; NM_002816.3:c.367C>T p.(Arg123*).

Subject 2 is the second child of non-consanguineous parents. The family history is unremarkable. The pregnancy was complicated by gestational diabetes, hydronephrosis and intrauterine growth restriction (IUGR). He was delivered at term via C-section. At birth, he showed respiratory distress and was in the intensive care unit (ICU) for 10 hours. At birth he showed, telecanthus, tented upper lip, myopathic face, bilateral thumb hypoplasia and femoral palm deformity. Both required surgery. Micropenis was noted in early childhood but is now resolved. Cardiac ultrasound revealed a small atrial septal defect (ASD) and patent ductus arteriosus (PDA) which both closed spontaneously. He initially failed his newborn screen but follow-up auditory brainstem responses were normal. At 6 months of age he was diagnosed with Eustachian tube dysfunction and pressure equalizer (PE) tubes were placed. He required G-tube feeding beginning at 18 months and he is still 100% dependent. At 5 years of age he was diagnosed with a seizure disorder. Magnetic resonance imaging (MRI) of the brain was considered normal. He was not able to sit independently until 8 months of age and to walk until 2 years and 7 months. He now requires a wheelchair. At last evaluation, at the age of 10 years and 7 months, he was able to pronounce many single words. He has been diagnosed with cortical visual impairment and is highly hyperopic. Ophthalmological examination at 3 years of age showed mildly abnormal optic nerve heads.

Using whole exome sequencing, a *de novo PSMD12* mutation was identified: Chr17(GRCh37):g.65337056A>C; NM_002816.3:c.1274T>G p.(Leu425*).

Subject 3 (11365.p1) is a male born to non-consanguineous parents of Caucasian European descent. His father's sibling has a history of broad spectrum autism with speech delay. Pregnancy was uncomplicated and he was delivered at 40 weeks gestation via vaginal delivery, with normal APGAR scores. He walked unaided at 15months, said his first word at 18 months, and his first phrase at 36 months. His medical records list a heart murmur at 3 years and an unspecified genital problem at 5 years.

At assessment at 14 years, he had a full scale IQ of 62 and a diagnosis of autism by Autism Diagnostic Interview Revised (ADI-R) and Autism Diagnostic Observation Schedule (ADOS). He was recruited to the Simons Simplex Collection where whole exome analysis identified a *de novo* nonsense mutation in the gene *PSMD12*.

Subject 4 is the fourth child of non-consanguineous parents. Family history is remarkable for an older brother who has intellectual disability, and hypotonia, and who was recently identified to have a rare, novel genetic syndrome related to the *TCF20* gene. Pregnancy was complicated by polyhydramnios towards the end and pregnancy induced hypertension at week 31. He was delivered at 39 weeks via spontaneous vaginal delivery with vacuum extraction. Birth weight was 3.2 kg and length was 50 cm. He had hyperbilirubinemia and breathing issues at birth but did not require oxygen. He also had chordee and a lymphangioma since birth.

In terms of his development, he sat on time, walked on time, and said "mama" and "dada" on time. He never had developmental regression. Developmental delays became apparent after one year of age. He began physical, occupational, and speech therapies and was placed in special education classes in preschool. Symptoms of Attention deficit hyperactivity disorder (ADHD) were apparent since he began walking, as per parental report. His health history is significant for gastroesophageal reflux disease (GERD), recurrent ear infections, velopharyngeal incompetence, cryptorchidism, frequent urination, innocent murmur, anisocoria, vision tracking issue and a pineal cyst found on brain MRI. Since age 3 he has had seizures characterized by his neurologist as reflex seizures. He has been diagnosed with autistic spectrum disorder.

In school, he currently performs two grade levels below expected. He repeated first grade and is currently in some mainstream classes with support and some special education classes in high school. His IQ is reportedly "just below average".

He presented to genetics at age 12 and was noted to have an asymmetric appearance to his face, mild hypertelorism, a large nose, mildly low set ears that are posteriorly rotated, and his bottom teeth were shifted to the left. He was noted to be tall and thin and did not make eye contact or answer questions when spoken to. He was flexible/hyperextensible at the wrists and elbows and was noted to have a small phallus and shawl scrotum. He had cutis marmorata on the legs and arms and lymphangioma on his left chest.

Previous work up included a normal chromosome microarray and Fragile X Syndrome testing. Two video EEGs were normal in 2006 and 2009. A holter monitor was

normal in 2009. A brain MRI from 2009 showed signal abnormality in the white matter of the centrum semiovale bilaterally, related punctate areas of gliosis versus demyelination. A lesion was observed in the region of the pineal gland, most likely representing a cyst.

Using whole exome sequencing, a *de novo PSMD12* mutation was identified: c.909-2A>G p.?, *de novo* heterozygous.

Subject 5 was 21 month of age at her last evaluation. She has a long standing history of developmental delay, failure to thrive. She has a history of arterial hypertension that requires treatment with captopril (ACE inhibitor). Genetics was initially consulted secondary to an abnormal echocardiogram that showed a large PDA with left to right shunt, hypoplastic isthmus and possible coarctation per notes. The infant had a repeat study which reportedly showed moderate sized PDA with left to right shunt, hypoplastic isthmus and possible coarctation that cannot be ruled out as PDA still open. PDA was ultimately surgically ligated.

Developmentally, she was delayed to reach her milestones: she rolled over at 9 months, crawled at 12 months, pulled to stand at 19 months, and was unable to walk at 21 months. She is currently able to use a few words.

On exam, she is small for her age, as she is just below the 3rd percentile for weight and length, and her head circumference is -2.7 SD below the mean. She is microcephalic and has dysmorphic features. The face appears elongated with prominent glabella with narrow forehead, hypertelorism, long philtrum and mild micrognathia. Her neck is short and her chest is broad. She has brachydactyly, and bridge creases.

She was diagnosed at 3 years of age with chronic renal disease stage I. Renal ultrasound showed hypoplastic kidneys and ectopic left kidney.

A computed tomography angiogram of chest and abdomen revealed: 1. a mild narrowing at the aortic isthmus measuring 5 x 4 mm; 2. a single unobstructed renal artery to the right kidney, as well as two unobstructed renal arteries to the left kidney, one arising from the descending aorta before the bifurcation, and the other arising from the right common iliac artery.

A chromosome microarray revealed a *de novo* deletion encompassing 1.3 megabases at chromosome 17q24.2.

Subject 6 was the product of a 37 week pregnancy complicated by slowed growth in the third trimester. At birth, he weighed 2.4 kg, and he was noted to have hypertelorism, simple cupped ears, micrognathia, hypospadias, and 2-3 toe syndactyly. At two weeks of age

he was found to have a patent ductus arteriosus (PDA) that required catheter-mediated occlusion, and which was complicated by a femoral thrombus. A mildly dysplastic tricuspid valve was noted, as were left ventricular trabeculations. He was also found to have a single functional kidney, with the other being atretic and multicystic. Hearing loss was identified by newborn screening, with moderate to severe loss in the right ear and intact hearing in the left ear. A temporal bone CT found stenotic external canals. A brain MRI revealed a moderate reduction in cerebral white matter volume, particularly posteriorly, with accompanying thinning of the posterior corpus callosum and periventricular hypomyelination. Dysmorphic appearing subcallosal frontal lobes were also noted, with interdigitation of gyri. Exotropia of the left eye was treated with patching and surgery. The family history was otherwise unremarkable. During infancy he had global developmental delay, hypotonia, failure to thrive and gastrointestinal reflux. He received physical, occupational, and speech therapy services, with steady developmental improvement, such that, by 3 years of age, he now walks independently, has a few words and attends school. A chromosome microarray revealed a *de novo* deletion encompassing 4 megabases at chromosome 17q23-24.2.

Subject 7 is the first child of non-consanguineous parents. The family history was unremarkable. The pregnancy was marked by severe growth retardation. He was delivered at 36 weeks via caesarean. At birth, he showed neonatal hypotonia and feeding difficulties, which required hospitalization for one month.

Later on, he still showed severe feeding difficulties. He was not able to walk until 18 months and showed severe speech delay. Evolution was marked by severe growth failure which required growth hormone (GH) therapy. Ophthalmological examination at 3 years of age showed myopia.

Precocious puberty was also noted and treated. At last evaluation, at the age of 13 years and 2 months, physical examination showed brachycephaly, thin lips, low set ears. Limbs examination showed bilateral 2-3 toes syndactyly. Subject 7 was able to pronounce many single words and understood simple orders. His neurological exam showed upper limbs tremor. He had severe chronic constipation. He was still treated by growth hormone for short stature. Hyperactivity and hands stereotypies were noted.

MRI of the brain was considered as normal. Abdominal and cardiac ultrasounds were normal.

A chromosome microarray revealed a *de novo* deletion encompassing 1.6 megabases at chromosome 17q23-24.2.

Subject 8 is the only child of non-consanguineous parents. Family history was unremarkable. Pregnancy was uncomplicated, with normal screening ultrasounds. She was delivered at 37 weeks of amenorrhea via vaginal delivery, with normal weight and OFC but height at 43.5 cm. As the height fell below -2 SD, investigations were done, leading to a diagnosis of central hypothyroidism, which was treated. She was referred at 5 months of age to a clinical geneticist. She presented with dysmorphic features including low set, posteriorly rotated ears, hypertelorism, down slanted palpebral fissures, wide nasal bridge, down-turned corners of the mouth. Cardiac and abdominal ultrasounds were normal. MRI of the brain was considered as normal. Subsequent evaluations showed normal motor milestones (walked independently at 10 months) but delayed speech.

At the last follow-up at age 5 years and 10 months, she presented learning difficulties, attention deficit, and persistent short stature below -2 SD despite appropriate thyroxin treatment. A chromosome microarray revealed a *de novo* deletion encompassing 1.19 megabases at chromosome 17q23-24.2

Subject 9 is the second child of non-consanguineous parents. Family history was unremarkable, save on the paternal branch, as the father has a first female cousin with autism and a maternal aunt with intellectual disability. Pregnancy was marked by an intrauterine growth restriction at 32 weeks, followed by a maternal fever and gastrointestinal illness at 36.5 weeks of gestation, which led to a cesarean section. Birth weight was 1.9 kg (< 1st percentile), length was 44.5 (1st percentile), and head circumference was 30 cm (3rd to 5th percentile). Echocardiogram at birth was normal. Renal sonogram revealed a horseshoe kidney. She stayed during her first 10 days in the neonatal intensive care unit with an initial oxygen requirement and she was treated with empiric antibiotics. She also needed nasogastric feeding initially.

Feeding issues began at 2 months, associated with gastro-esophageal reflux, and oral aversion. At this age, she was also evaluated by a neurologist, due to her small head size. She had a poor muscle tone.

In terms of her development, her delay is global, as it concerns gross motor, fine motor, and speech. She reached her milestones with delay: she rolled at 7.5 months, babbled at 9 months, sat at 11 months, commando crawled at 12.5 months, high crawled at 17 months, and walked at 26 months. At 5 years and 10 months, she could use 50 to 60 single words, but could not speak in 2-3 word combinations yet. The poor muscular tone noted at birth was

confirmed at 5 months, as she showed hypotonia and head lag, whereas deep tendon reflexes were normal. At 12 months, she still exhibited mild hypotonia. At 4 years and 6 months she presented slightly wide-based gait, normal deep tendon reflexes and had some problems with her balance and coordination.

Growth delay was observed at 5 months (weight and head circumference < 3rd percentile, length 5-10th percentile), and confirmed at 12 months (weight at 3rd percentile, length at 10-25th percentile, and head circumference at 5-10th percentile).

She presents dysmorphic features: frontal bossing and mild parietal bossing, mild brachycephaly, large anterior fontanelle, prominent forehead, mild bitemporal narrowing, pseudohypertelorism, normal chin width with retrognathia, square pinnae with attached lobules, low hanging columella, depressed nasal bridge, short and mildly smooth philtrum, high arched palate (U-shaped), absent Cupid's bow, small mouth, and mildly downturned mouth corners. She has a short sternum, and a higher nipple line than usual. Fingers and hands are mildly triangular, with as slightly puffy dorsum, and decreased depth of creases on R, while thumbs are longer than usual. She also has a bilateral 2-3 toe syndactyly, narrow feet and hyperextension at knees.

A strabismus was corrected by surgery.

Analysis of a muscle biopsy revealed a decrease in staining of mitochondrial complex 1, albeit with normal enzyme activities (complex I-IV). Whole-exome sequencing did not point to a disease with known secondary mitochondrial dysfunction, and no significant mtDNA finding was done. A single autosomal recessive *SUCLA2* change was found with varying *in silico* predictions, as well as a maternally inherited change in *RAI1*, unlikely to be pathogenic. Array CGH showed a *de novo* microdeletion on 17q.

Subject 10 is a 9-year-old child of consanguineous parents (second-degree cousins). The rest of her family history is unremarkable. Her mother presented preeclampsia since the fourth month of pregnancy and was delivered at 34 weeks of pregnancy by caesarean section due to oligohydramnion. Her birth weight was 2.100 grams, and birth height was 46 cm. She had hypertelorism, low set ears, high forehead, high-arched palate, wide nose, hypotonia and right side hydronephrosis reported on ultrasound. She has developmental delay: she was not able to walk until she was 16 months old; speech started at three years of age, and she now uses many words but is still unable to use phrases. She had a tonic convulsion episode at 6 years of age. Precocious puberty is under treatment; at last evaluation, at the age of 9 years, she had pubic hair. Ophthalmological examination showed strabismus and left eye coloboma.

Array CGH showed a *de novo* microdeletion on 17q24.2 which turned out to be a complex rearrangement as shown in Figure S10.

SUPPLEMENTAL FIGURES S1-10 AND LEGENDS

Figure S1. Morphological anomalies in subjects 1[a], 2 [a], 7, 9 and 10.
Consent for the publication of photographs was obtained for the five subjects. Note microretrognathia, strabismus, and low set ears (A), and right thumb agenesis (F) in Subject 1; low set ears, telecanthus, and bilateral thumb hypoplasia in Subject 2 (C, D, and F); mild brachycephaly, prominent forehead, mild bitemporal narrowing, short philtrum, small mouth, mildly downturned mouth corners, mildly triangular fingers with long thumbs and a bilateral 2-3 toe syndactyly in Subject 9 (D, E, H and I); brachycephaly, thin lips, and low set ears in Subject 7 (J and K); and hypertelorism, low set ears, high forehead, high arc palate, and wide nose in Subject 10 (L).
[a] *Photographs of Subjects 1 and 2 are presented also in Figure 1, but they are shown again to enable direct comparisons.*

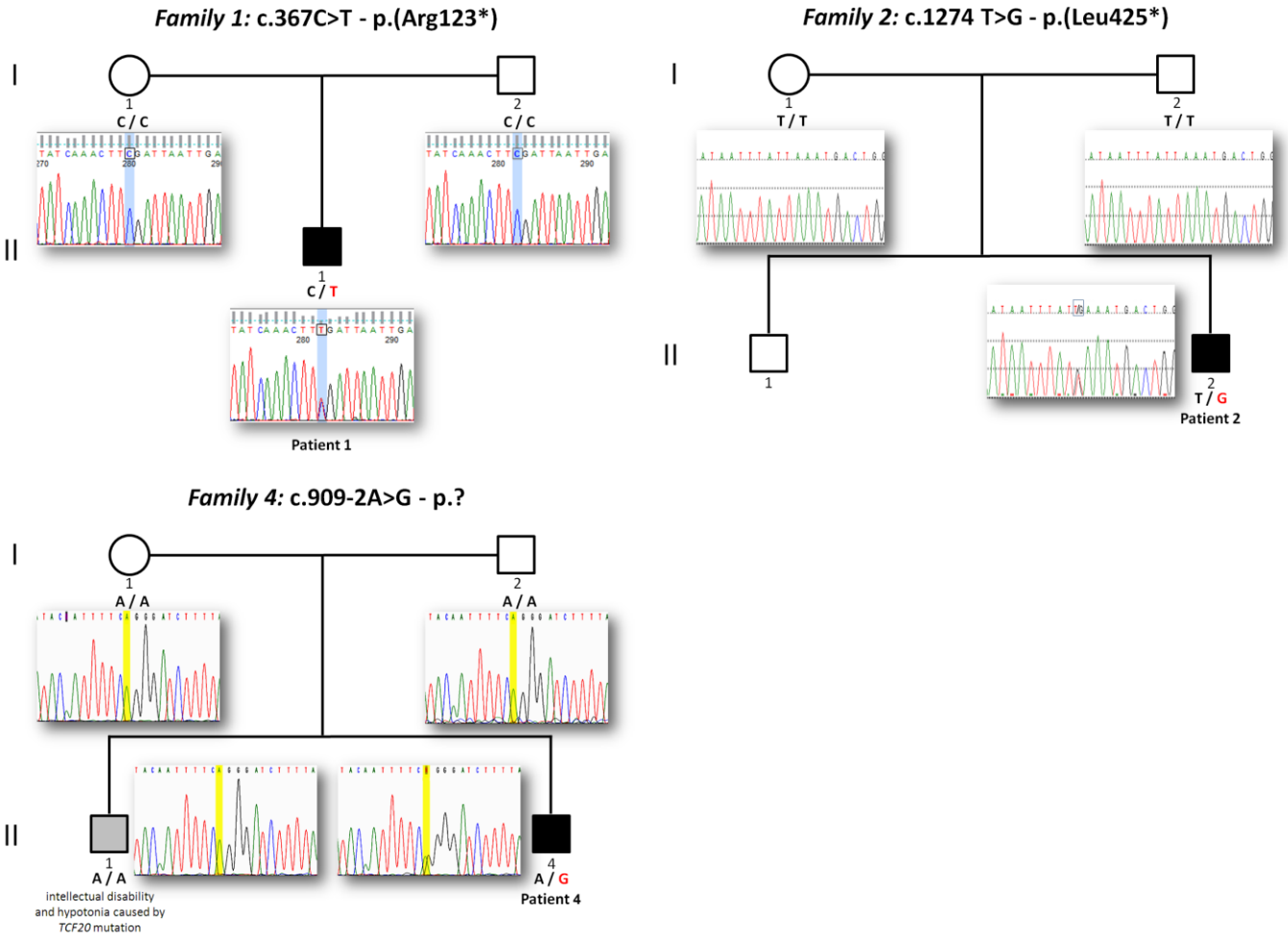

Figure S2. Segregation analysis of *PSMD12* mutations. [a]

This figure shows the genealogical trees of subjects 1, 2 and 4. Genotypes identified by whole exome sequencing were validated by Sanger sequencing. Electropherograms related to mutations found by Sanger sequencing figure below each individual of the trios whenever traces were available.

[a] In Family 3, the variant c.601C>T p.(Arg201*)was confirmed using custom Molecular Inversion Probes (MIP) -designed with targeting arms flanking regions of interest- and followed by sequencing on an Illumina MiSeq.

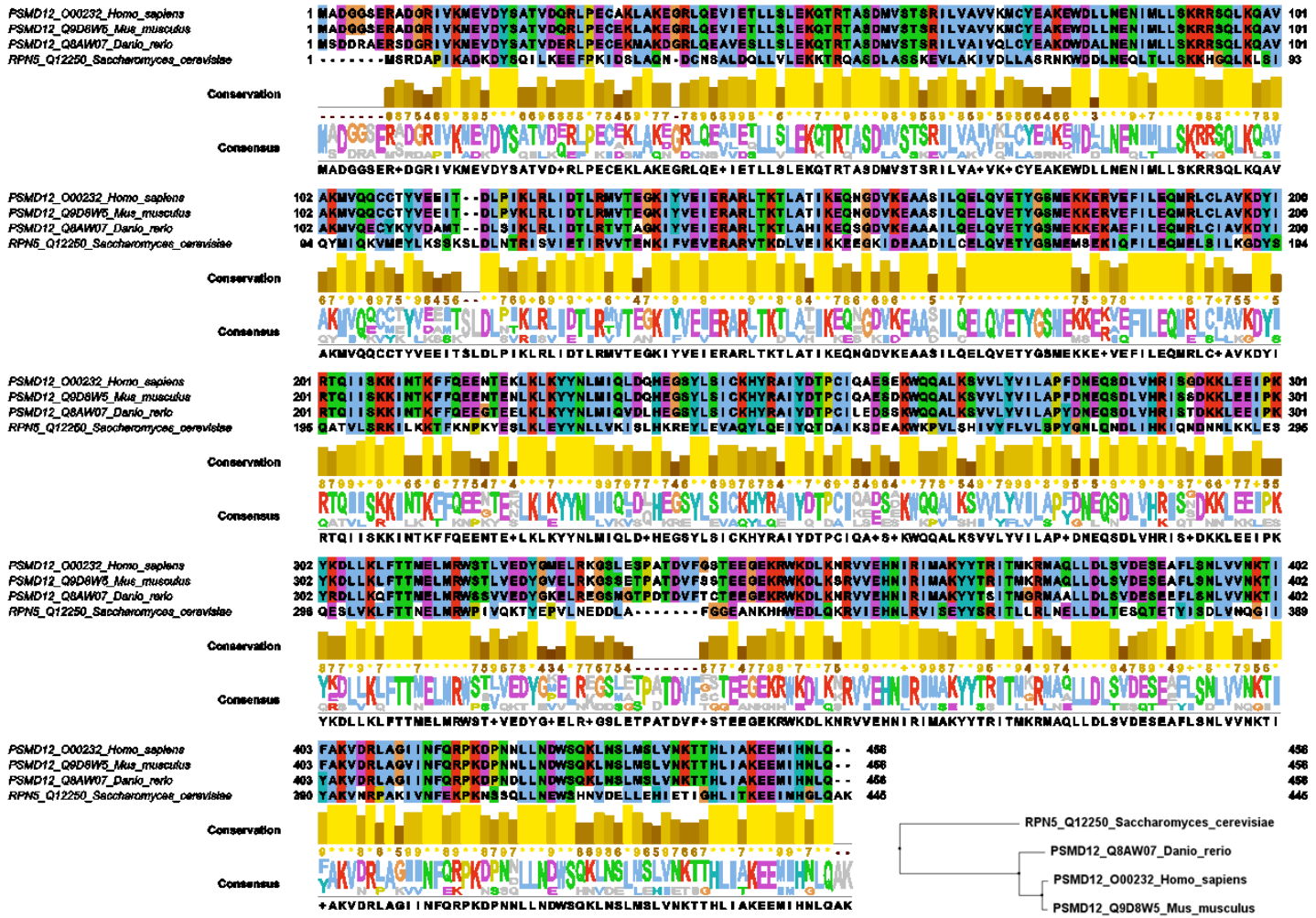

Figure S3. Multiple sequence alignment of the PSMD12/RPN5 protein from four organisms: Homo Sapiens, Mus musculus, Danio rerio, Saccharomyces cerevisiae.

The alignment has been performed using Clustal Omega and visualized using JalView. Sequences are indicated using the Uniprot identifiers. Colors correspond to consensus-based coloring of ClustalX multiple alignments. The figure shows a high conservation of PSMD12 (RPN5) across species.

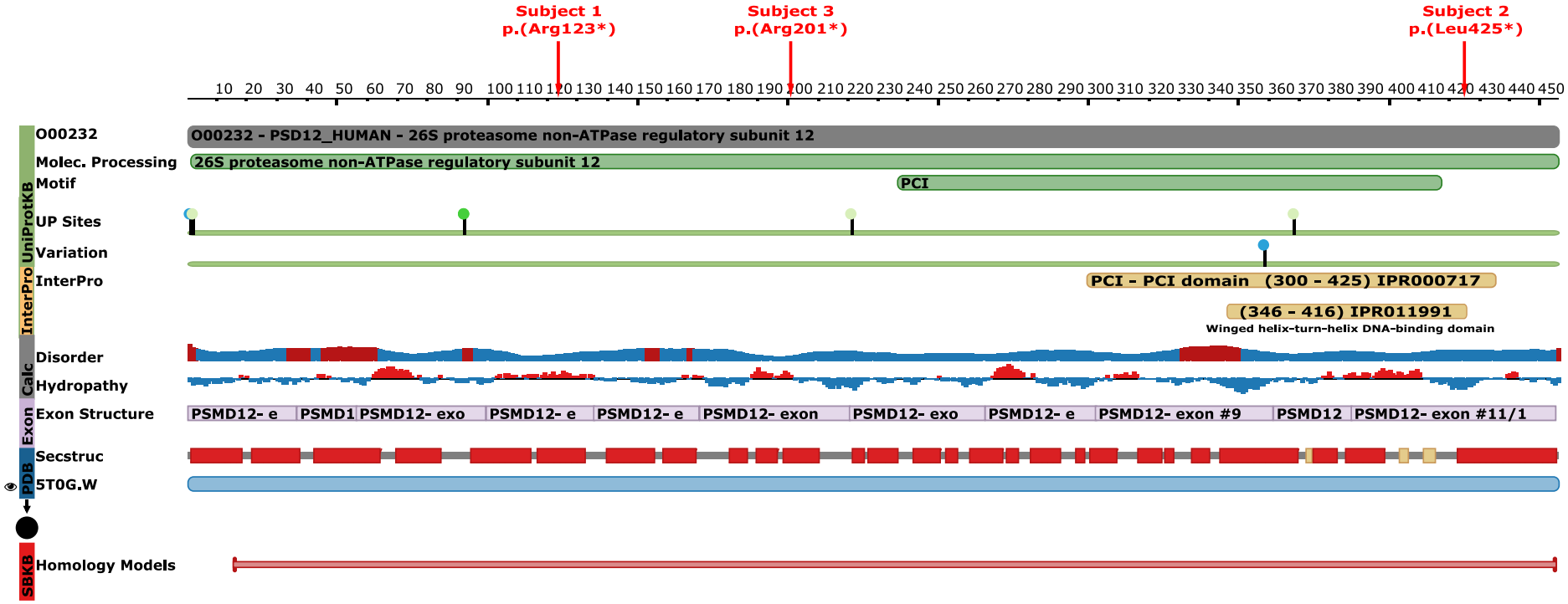

Figure S4. Protein feature view of 26S proteasome non-ATPase regulatory subunit 12.

Image adapted from the RCSB PDB (www.rcsb.org) of PDB entry O00232 (PSD12_HUMAN) [1]. The three nonsense single nucleotide variants found in subjects of our series, and indicated on top of the figure by red arrows, disrupt the proteasome–COP9 signalosome (PCI). Vertical color bars on the left side indicate data provenance: in green data from UniProtKB; in yellow data from InterPro; in grey data calculated using BioJava with protein disorder predictions based on JRONN; in lilac data representing the genomic exon structure projected onto the UniProt sequence; in blue data from PDB (Secstruc: Secondary structure) projected from representative PDB entries onto the UniProt sequence; in red data combining ranges of Homology Models from SBKB and the Protein Model Portal.

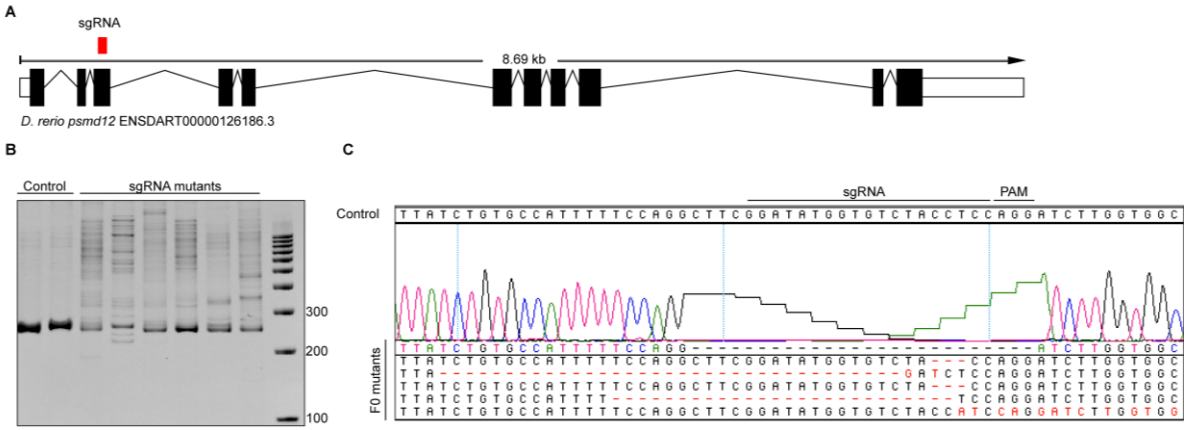

Figure S5. Reagents for CRISPR Cas9 genome editing in zebrafish embryos.

(A) Sketch of *D. rerio psmd12*; showing coding exons (black boxes) and untranslated regions (white boxes). The position of the target of CRISPR sgRNA (red box) is shown. (B) Polyacrylamide gel electrophoresis (15% PAGE; BioRad) shows the presence of heteroduplexes indicating targeting events in F0 CRISPR embryos (C) Representative Sanger sequencing traces of un-injected control embryos and F0 embryos injected with psmd12 sgRNA3 and Cas9 protein show insertion and or deletion events in the target region. The protospacer adjacent motif (PAM) sequence for sgRNA is shown.

A.

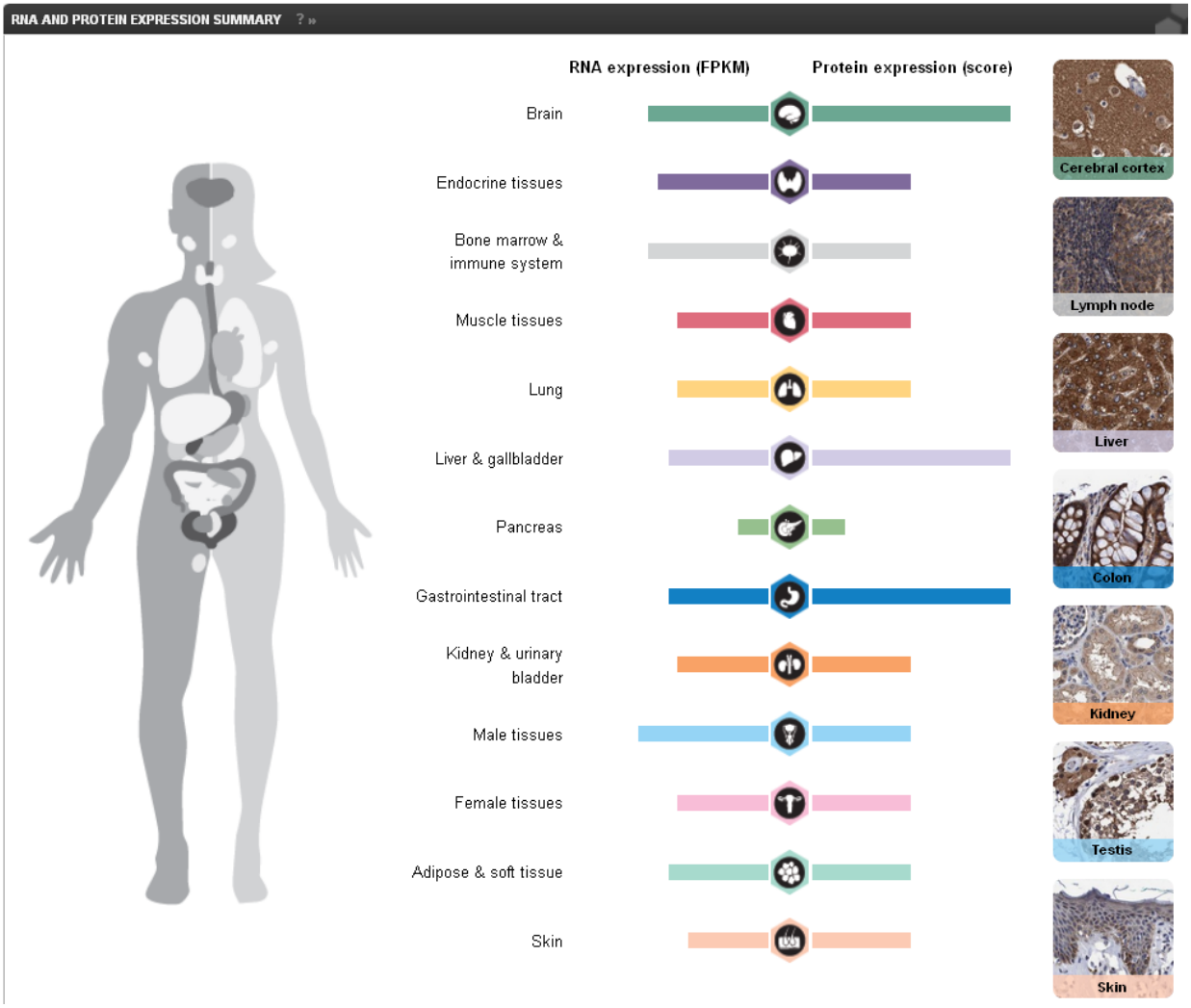

B.

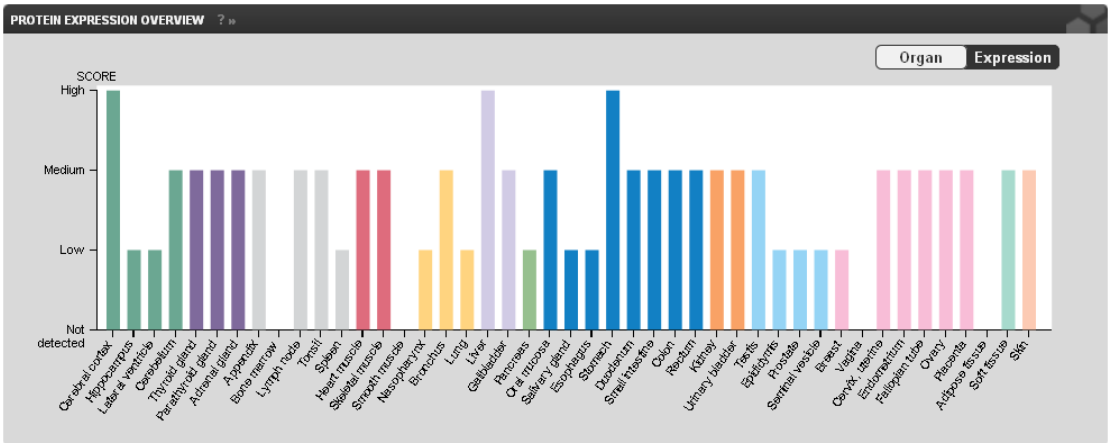

Figure S6. Expression of *PSMD12* in human tissues.

Overview from the Human Protein Atlas [2] (http://www.proteinatlas.org/ENSG00000197170-PSMD12/tissue) shows a wide RNA expression and distribution of PSMD12 protein levels in the human body. **(B)**, Protein levels are particularly increased in brain, liver/gallbladder and gastrointestinal tract and **(C)**, more especially in cerebral cortex.

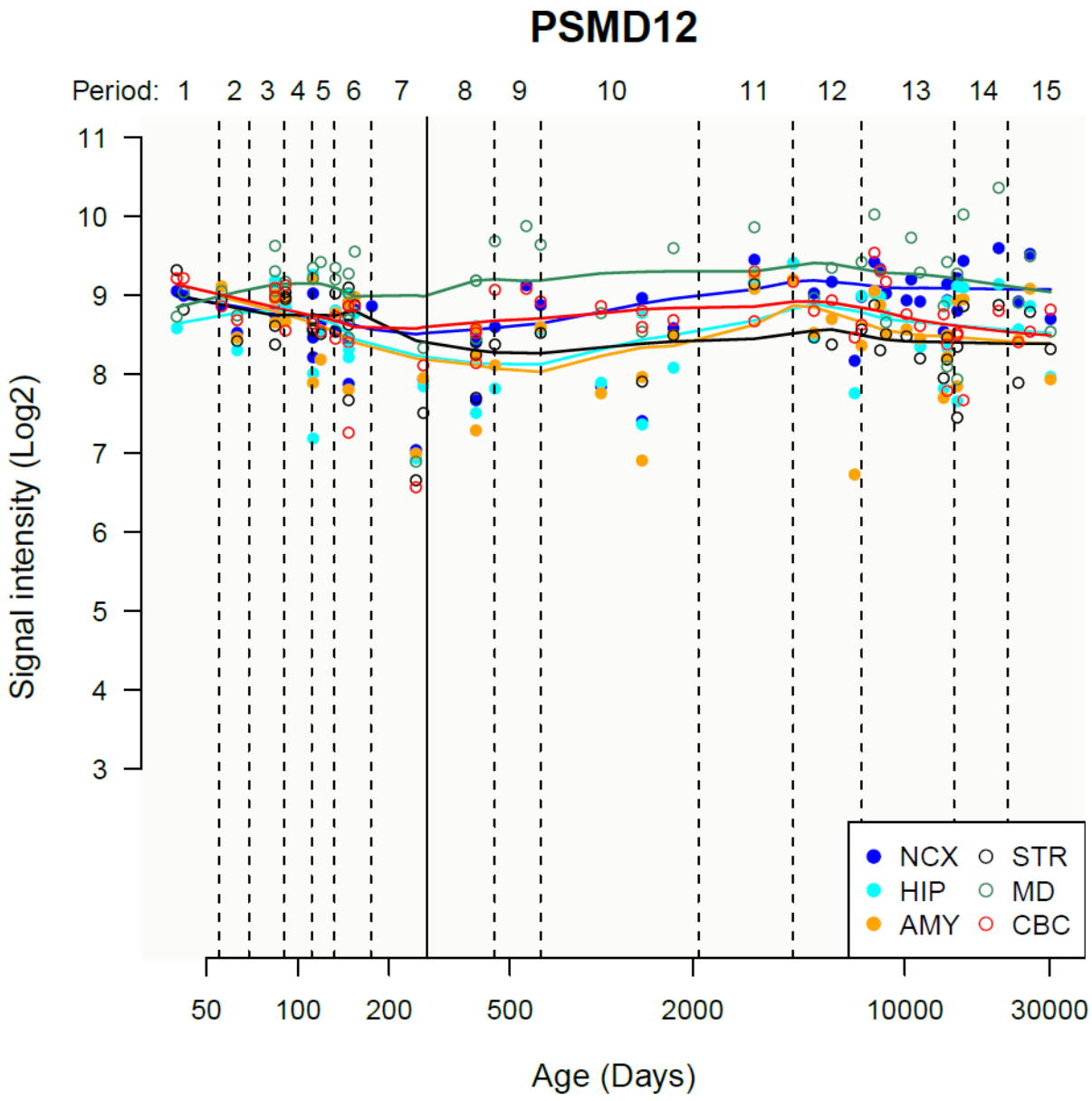

Figure S7. Expression of *PSMD12* in human brain.

Data were extracted from the Human Brain Transcriptome database [3; 4] (http://hbatlas.org/). The dynamic gene expression of *PSMD12* is high and steady along entire development and adulthood in the human cerebellar cortex (CBC), mediodorsal nucleus of the thalamus (MD), striatum (STR), amygdala (AMY), hippocampus (HIP) and 11 areas of neocortex (NCX).

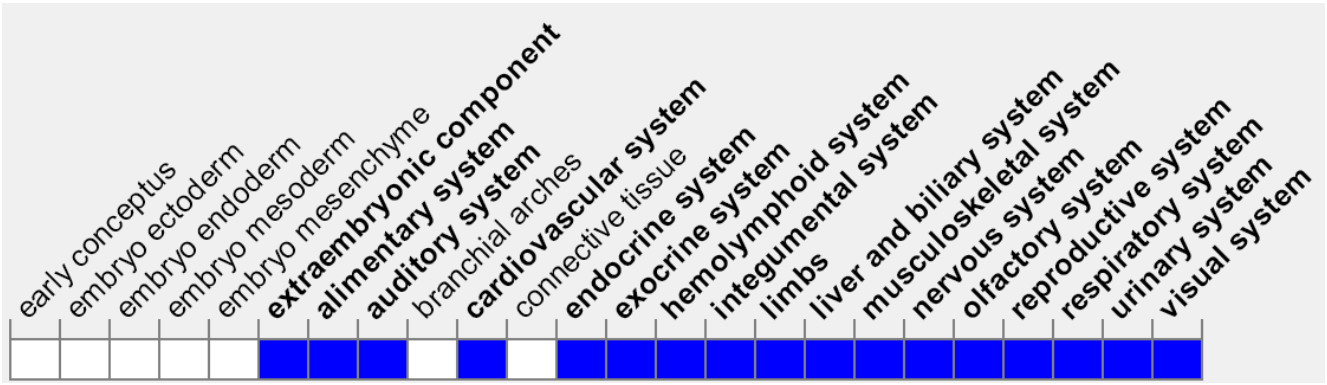

Figure S8. Expression of *PSMD12* in mouse tissues.

Expression data for this paper were retrieved from the Gene Expression Database (GXD) [5], Mouse Genome Informatics Web Site. World Wide Web (URL: http://www.informatics.jax.org). [November, 2016]. Expression overview in mouse confirms the wide RNA expression and distribution of PSMD12 protein levels in the body (http://www.informatics.jax.org/marker/MGI:1914247).

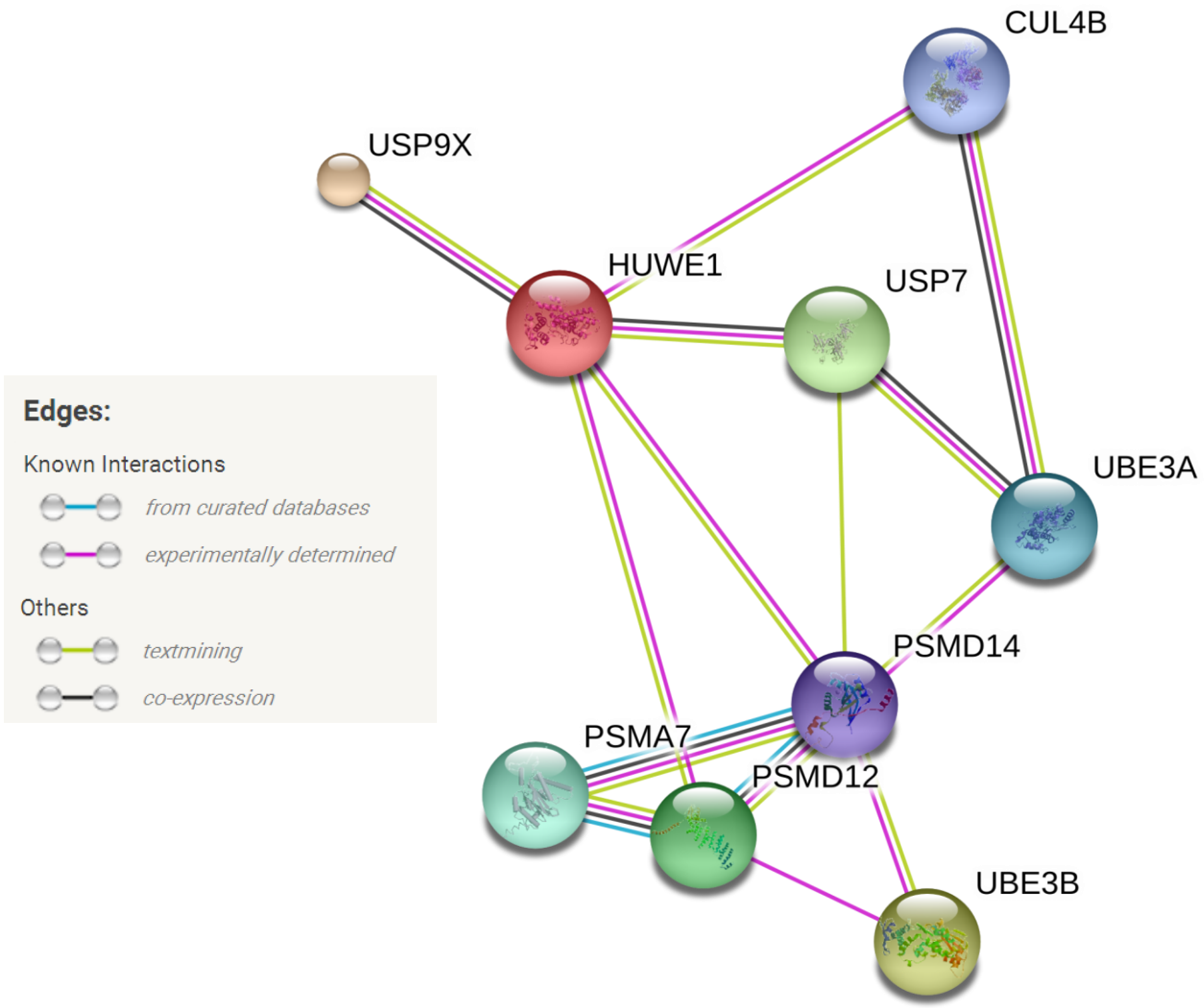

Figure S9. Interactions between PSMD12 and other proteins of Ubiquitin/Proteasome signaling pathway involved in intellectual disabilities.

Interaction between UPS proteins known (UBE3A, UBE3B, HUWE1, USP7, USP9X, CUL4B) or suspected (PSMA7, PSMD14) to be involved in intellectual disabilities were determined according to String Database 10.0 [6].

Network nodes represent proteins: small nodes indicate protein of unknown 3D structure; large nodes indicate that some 3D structure is known or predicted; colored nodes show query proteins and first shell of interactors. Edges represent protein-protein associations: associations are meant to be specific and meaningful, i.e. proteins jointly contribute to a shared function; this does not necessarily mean they are physically binding each other.

Complex rearrangement 1:
chr17:65480260(-) ➔ chr17:65711757(+), *Alu-Alu* mediated, , microhomology in purple

GGAGTTCGAGACCAGCCTAACCAACATGGAGAAACCCCGTCTCTACTAAAAATACAAAATAAGCCA
GGCATGGTGGTACATGCCTGTAATGCCAGCTACTTGGGAGGCTG
GGAGTTCGAGACCAGCCTAACCAACATGGAGAAACCCCGTCTCTACTAAAAATACAAAATAAGCCA
GGCATGGTGGTACATGCCTGTAATGCCAGCTACTTGGGAGGCTG
GGAGTTCGAGACCAACCTGGCCAACATGGTGAAACCCCGTCTCTACTAAAAATACAAAAATTAGCC
AGGTGTGGGGTGGGTGCCTCTAATCCCAGCTACTCGGGAGGCTG

AGG**CAGGAGAATCGCTTGAACC**TGGGAGGTGGAGGTTGCAGT----
GAGCCAAGATCATGCCACGGCACTCCAGCCTGGGCAACAAGAGCAAAACTCCACCTCAAAAAAAAA
AAAAA
AGG**CAGGAGAATCGCTTGAACC**CGGGGGGCAGAGGTTGCAGGTTGCAGAGAGCCGAGATTGTGCCA
TTGCACTCCAGCCTTCGTGACAAGAGTGAACCTCTGTCTCAAAAAAGAAAAAAA
AGA**CAGGAGAATCGCTTGAACC**CGGGGGGCAGAGGTTGCAGGTTGCAGAGAGCCGAGATTGTGCCA
TTGCACTCCAGCCTTCGTGACAAGAGTGAACCTCTGTCTCAAAAAAGAAAAAAA

Complex rearrangement 2:
chr17: 65090765(+) ➔ 65513478(-), microhomology in purple

ATCTATTAAGTGTGCAATAGCATTGTATGTTTAAAAAAACACAATGTATAAAGGCAAG**CAT**GGTGT
CACATGCCTGTAGGCCCAGCTACTTGGGAGGCTGAAGAGGGAGGATCATTTGAGCCCATGAG
ATCTATTAAGTGTGCAATAGCATTGTATGTTTAAAAAAACACAATGTATAAAGGCAAG**CAT**TTCCC
TTGGATGTGGAATTACTGGGTCACATGGTAACAACATGTTTGACCATTTGAGGAACTGTCAG
ATTATGAATAATGCTGCTATGAGTATTTGTGGGTGAGTCTTTTGAGGACGTATGTTTT**CAT**TTCCC
TTGGATATGGAATTACTGGGTCACATGGTAACAACATGTTTGACCATTTGAGGAACTGTCAG

Figure S10. Details of the CNV deletion observed in Subject 10.

Long range PCR in Subject 10's genomic DNA yielded an ~620 kb deletion-specific junction fragment. Subsequent sequencing revealed a complex rearrangement consisting of a 389,495 bp deletion (chr17:65,090,765-65,480,260) with a CAGGAGAATCGCTTGAACC microhomology at the first junction and a 198,279 bp deletion (chr17:65,513,478-65,711,757) with a CAT microhomology at the second junction; both deletions are separated by a neutral copy-number genomic segment of approximately 33 kb that is oriented directly with respect to the reference human genome sequence (Genome Browser GRCh37/hg19).

SUPPLEMENTAL TABLES S2-6

Table S2. Clinical features of the subjects described with Human Phenotype Ontology (HPO) terms.

Family 1	Family 2	Family 3	Family 4	Family 5	Family 6	Family 7	Family 8	Family 9	Family 10
Subject 1 – HUGODIMS	**Subject 2 - Boston Children's Hospital**	**Subject 3 - SSC**	**Subject 4 - BG**	**Subject 5 - BG**	**Subject 6 - BG**	**Subject 7 – CHU de Toulouse**	**Subject 8 - CHU de la Réunion**	**Subject 9 - BG**	**Subject 10 - BG**
Abnormality of the cardiovascular system (HP:0001626) truncus arteriosus (HP:0001660) Ventricular septal defect (HP:0001652) atrial septal defect (HP:0001631) Hypoplastic aortic arch (HP:0012304) Patent ductus arteriosus (HP:0001643) Abnormality of the kidney (HP:0000077) Crossed fused renal ectopia (HP:0004736) Abnormality of male external genitalia (HP:0000032) Hypospadias (HP:0000047) Abnormality of the upper limb (HP:0002817) Aplasia/Hypoplasia of the thumb (HP:0009601) Intellectual disability (HP:0001249) Motor delay (HP:0001270) Delayed speech and language development (HP:0000750) Muscular hypotonia (HP:0001252) Behavioral abnormality (HP:0000708) Hearing impairment (HP:0000365) Feeding difficulties (HP:0011968) Abnormality of the eye (HP:0000478) Horizontal nystagmus	Birth length less than 3rd percentile (HP:0003561) Abnormality of the cardiovascular system (HP:0001626) Patent ductus arteriosus (HP:0001643) Abnormality of the kidney (HP:0000077) Fetal pyelectasis (HP:0010945) Abnormality of the ureter (HP:0000069) Urinary retention (HP:0000016) Abnormality of male external genitalia (HP:0000032) Micropenis (HP:0000054) Abnormality of the upper limb (HP:0002817) Aplasia/Hypoplasia of the thumb (HP:0009601) Sacral dimple (HP:0000960) Tracheomalacia (HP:0002779) Laryngeal cleft (HP:0008751) Intellectual disability (HP:0001249) Motor delay (HP:0001270) Delayed speech and language development (HP:0000750) Behavioral abnormality (HP:0000708) Autistic behavior (HP:0000729) Seizures (HP:0001250) Hearing impairment (HP:0000365) Feeding difficulties (HP:0011968)	Abnormality of the cardiovascular system (HP:0001626) Heart murmur (HP:0030148) Abnormality of male external genitalia (HP:0000032) Intellectual disability (HP:0001249) Delayed speech and language development (HP:0000750) Behavioral abnormality (HP:0000708) Autistic behavior (HP:0000729)	Abnormality of male external genitalia (HP:0000032) Cryptorchidism (HP:0000028) Micropenis (HP:0000054) Shawl scrotum (HP:0000049) Intellectual disability (HP:0001249) Muscular hypotonia (HP:0001252) Behavioral abnormality (HP:0000708) Autistic behavior (HP:0000729) Seizures (HP:0001250) Abnormality of the eye (HP:0000478) Impaired smooth pursuit (HP:0007772) Pineal cyst (HP:0012683) Abnormality of the outer ear (HP:0000356) Low-set ears (HP:0000369) Posteriorly rotated ears (HP:0000358) Abnormality of the face (HP:0000271) Facial asymmetry (HP:0000324) Hypertelorism (HP:0000316) Prominent nose (HP:0000448) Cutis marmorata (HP:0000965) Lymphangioma (HP:0100764)	Microcephaly (HP:0000252) Abnormality of the cardiovascular system (HP:0001626) Patent ductus arteriosus (HP:0001643) coarctation of aorta (HP:0001680) Abnormality of the kidney (HP:0000077) Hydronephrosis (HP:0000126) Renal hypoplasia (HP:0000089) Ectopic kidney (HP:0000086) Intellectual disability (HP:0001249) Motor delay (HP:0001270) Delayed speech and language development (HP:0000750) Microretrognathia (HP:0000308) Abnormality of the mandible (HP:0000277) Abnormality of the face (HP:0000271) Hypertelorism (HP:0000316) Long philtrum (HP:0000343) Hypertension (HP:0000822)	Growth delay (HP:0001510) Abnormality of the cardiovascular system (HP:0001626) Patent ductus arteriosus (HP:0001643) Left ventricular noncompaction cardiomyopathy (HP:0011664) Hypoplastic tricuspid valve (HP:0011573) Abnormality of the kidney (HP:0000077) unilateral kidney agenesis (HP:0000122) Abnormality of male external genitalia (HP:0000032) Hypospadias (HP:0000047) Abnormality of the lower limb (HP:0002814) 2-3 toe cutaneous syndactyly (HP:0005709) Intellectual disability (HP:0001249) Motor delay (HP:0001270) Delayed speech and language development (HP:0000750) Muscular hypotonia (HP:0001252) Hearing impairment (HP:0000365) Feeding difficulties (HP:0011968) Cerebral atrophy (HP:0002059) Cerebral hypomyelination (HP:0006808) Pineal cyst (HP:0012683) Abnormality of the eye (HP:0000478)	Growth delay (HP:0001510) Birth length less than 3rd percentile (HP:0003561) Abnormality of the lower limb (HP:0002814) 2-3 toe cutaneous syndactyly (HP:0005709) Sacral dimple (HP:0000960) Intellectual disability (HP:0001249) Motor delay (HP:0001270) Delayed speech and language development (HP:0000750) Muscular hypotonia (HP:0001252) Behavioral abnormality (HP:0000708) Hyperactivity (HP:0000752) Retrognathia (HP:0000278) Abnormality of the mandible (HP:0000277) Feeding difficulties (HP:0011968) Abnormality of the eye (HP:0000478) Myopia (HP:0000545) Abnormality of the face (HP:0000271) Short philtrum (HP:0000322) Thin upper lip vermilion (HP:0000219) Constipation (HP:0002019) Tremor (HP:0001337) Aplasia cutis congenita over the scalp vertex (HP:0004471)	Growth delay (HP:0001510) Birth length less than 3rd percentile (HP:0003561) Intellectual disability (HP:0001249) Delayed speech and language development (HP:0000750) Behavioral abnormality (HP:0000708) Hyperactivity (HP:0000752) Abnormality of the outer ear (HP:0000356) Low-set ears (HP:0000369) Posteriorly rotated ears (HP:0000358) Abnormality of the face (HP:0000271) Hypertelorism (HP:0000316) Down-slanted palpebral fissures (HP:0000494) Wide nasal bridge (HP:0000431) Downturned corners of mouth (HP:0002714) Central hypothyroidism (HP:0011787)	Growth delay (HP:0001510) Congenital microcephaly (HP:0011451) Birth length less than 3rd percentile (HP:0003561) Abnormality of the kidney (HP:0000077) Ectopic kidney (HP:0000086) Horseshoe kidney (HP:0000085) Abnormality of the lower limb (HP:0002814) 2-3 toe cutaneous syndactyly (HP:0005709) Short sternum (HP:0000879) Triangular shaped phalanges of the hand (HP:0009774) Intellectual disability (HP:0001249) Motor delay (HP:0001270) Delayed speech and language development (HP:0000750) Muscular hypotonia (HP:0001252) Feeding difficulties (HP:0011968) Abnormality of the eye (HP:0000478) Strabismus (HP:0000486) Myopia (HP:0000545) Abnormality of the outer ear (HP:0000356) Microretrognathia (HP:0000308) Abnormality of the mandible (HP:0000277) Abnormality of the face (HP:0000271)	Birth length less than 3rd percentile (HP:0003561) Macrocephaly (HP:0000256) Hydronephrosis (HP:0000126) Abnormality of the kidney (HP:0000077) Precocious puberty (HP:0000826) Puberty and gonadal disorders (HP:0008373) Coloboma (HP:0000589) Strabismus (HP:0000486) Abnormality of the eye (HP:0000478) Intellectual disability (HP:0001249) Motor delay (HP:0001270) Delayed speech and language development (HP:0000750) Muscular hypotonia (HP:0001252) Behavioral abnormality (HP:0000708) Seizures (HP:0001250) Low-set ears (HP:0000369) Posteriorly rotated ears (HP:0000358) Abnormality of the outer ear (HP:0000356) High forehead (HP:0000348) Abnormality of the face (HP:0000271)

(HP:0000666) Strabismus (HP:0000486) Abnormality of the outer ear (HP:0000356) Low-set ears (HP:0000369) Posteriorly rotated ears (HP:0000358) Microretrognathia (HP:0000308) Abnormality of the mandible (HP:0000277) Recurrent pneumonia (HP:0006532)	Abnormality of the eye (HP:0000478) Cortical visual impairment (HP:0100704) Abnormality of the optic nerve (HP:0000587) Abnormality of the outer ear (HP:0000356) Low-set ears (HP:0000369)				Exotropia (HP:0000577) Abnormality of the outer ear (HP:0000356) Low-set ears (HP:0000369) Abnormality of the face (HP:0000271) Hypertelorism (HP:0000316)			Hypertelorism (HP:0000316) Frontal bossing (HP:0002007) Brachycephaly (HP:0000248) Wide anterior fontanel (HP:0000260) Prominent forehead (HP:0011220) Narrow forehead (HP:0000341) Low hanging columella (HP:0009765) Bulbous nasal tip (HP:0000414) Smooth philtrum (HP:0000319) Short philtrum (HP:0000322) Absent cupid's bow (HP:0010800) Narrow mouth (HP:0000160) High palate (HP:0000218) Muscular hypotonia (HP:0001252) Abnormality of the nipple (HP:0004404)	

Table S3. Main phenotypic abnormalities referring to HPO shared by at least three subjects.

HPO ID	Number of subjects concerned	HPO term
HP:0001249	10/10	Intellectual disability
HP:0000750	9/10	Delayed speech and language development
HP:0000271	7/9	Abnormality of the face
HP:0000356	7/9	Abnormality of the outer ear
HP:0000708	7/9	Behavioral abnormality
HP:0000478	7/9	Abnormality of the eye
HP:0001270	7/10	Motor delay
HP:0001252	6/9	Muscular hypotonia
HP:0000077	6/9	Abnormality of the kidney
HP:0000369	6/9	Low-set ears
HP:0000032	5/6	Abnormality of male external genitalia
HP:0011968	5/9	Feeding difficulties
HP:0000316	5/9	Hypertelorism
HP:0001626	5/9	Abnormality of the cardiovascular system
HP:0003561	5/10	Birth length less than 3rd percentile
HP:0001643	4/9	Patent ductus arteriosus
HP:0000277	4/9	Abnormality of the mandible
HP:0000358	4/9	Posteriorly rotated ears
HP:0001510	4/10	Growth delay
HP:0000308	3/9	Microretrognathia
HP:0000729	3/9	Autistic behavior
HP:0001250	3/10	Seizures
HP:0005709	3/10	2-3 toe cutaneous syndactyly
HP:0002814	3/10	Abnormality of the lower limb
HP:0000365	3/10	Hearing impairment

Table S4. Candidate genes inferred from trio-based whole-exome sequencing and array CGH data.

Sample	Method/finding	Putative *de novo* mutations	Newly Hemizygous genotype	Newly Homozygous genotype	Compound Heterozygous genotype
Subject 1	WES/SNV	*PSMD12* *ABCA2, TPR*	0	0	0
Subject 2	WES/SNV	*PSMD12*	0	0	0
Subject 3	WES/SNV	*PSMD12*	0	0	0
Subject 4	WES/SNV	*PSMD12*	0	0	0
Subject 5	aCGH/CNV (deletion)	*PSMD12* *PITPNC1, NOL11, BPTF*	ND	ND	ND
Subject 6	aCGH/CNV (deletion)	*PSMD12* *APOH, CAEP112, AXIN2, RGS9, GNA13, LOC146880, LPRC37A3, TEX2, MILR1, POLG2, SMURF2, DDX5, CEP95, PLEKHM1P, HELZ, CACNG1, CACNG4, CACNG5, PRKCA, PITPNC1, NOL11, BPTF, C17orf58, AMZ2, LOC440461, SLC16A6, ARSG*	ND	ND	ND
Subject 7	aCGH/CNV (deletion)	*PSMD12* *HELZ, CACNG1, CACNG4, CACNG5, PRKCA, PITPNC1, NOL11, BPTF, C17orf58*	ND	ND	ND
Subject 8	aCGH/CNV (deletion)	*PSMD12* *HELZ, CACNG1, CACNG4, CACNG5, PRKCA, PITPNC1, NOL11, C17orf58*	ND	ND	ND
Subject 9	aCGH/CNV (deletion)	*PSMD12* *PITPNC1, NOL11, BPTF, C17orf58, KPNA2*	0	0	*SUCLA2*
Subject 10	aCGH/CNV (deletion)	*PSMD12* *PITPNC1, HELZ*	0	0	*SUCLA2*

WES : whole-exome sequencing ; aCGH: array comparative genomic hybridization; SNV: single nucleotide variant; CNV: copy number variation

Table S5. *In silico* predictions of pathogenicity for the *PSMD12* splice site variant found in the case series.

Below the table is shown the summary of this prediction, according to the Alamut Visual v.2.7. program (Integrative Biosoftware).

Subject	HGVSc [δ,*] (exon)	HGVSp [δ] (amino acids)	SSF Score* (wt–var)	MaxEnt [±] Score (wt–var)	NNS Score [¶] (wt–var)	GS [#] Score (wt–var)	HSF [¥] Score (wt–var)
Subject 4	c.909-2A>G (intron 8)	p.?	83.91–0	3.65-0	0-0	0-0	87.22-0

[δ] HGVSc/HGVSp: coding DNA/protein variant described according to the nomenclature established by the Human Genome Variation Society.
* Nomenclature HGVS V2.0 according to mRNA reference sequence NM_002816.3. Nucleotide numbering uses +1 as the A of the ATG translation initiation codon in the reference sequence, with the initiation codon as codon 1.
* SSF: Splice Site Finder-like, wt: wild-type, var: variant; [±] MaxEnt; [¶] NNS: NNSplice; [#] GS: Gene Splicer; [¥] HSF: Human Splicing Finder

Table S6. List of primers used for CRISPR Cas9 genome editing in zebrafish embryos.

Name of the primer	Sequence (5'-3')
psmd12_sgRNA_F	TAATACGACTCACTATAG**GGATATGGTGTCTACCTCC**
psmd12_sgRNA_R	TTCTAGCTCTAAAAC**GGAGGTAGACACCATATCC**
psmd12_sgRNA_PCR_F	TTGTGTGTGTTTAAAGGATGGC
psmd12_sgRNA_PCR_R	TAGCAGCATGATGTTTTCGTTC

Sequences of the CRISPR guide RNA targets are given in bold

SUPPLEMENTAL REFERENCES

1. Drew, H.R., Wing, R.M., Takano, T., Broka, C., Tanaka, S., Itakura, K., and Dickerson, R.E. (1981). Structure of a B-DNA dodecamer: conformation and dynamics. Proceedings of the National Academy of Sciences of the United States of America 78, 2179-2183.
2. Uhlen, M., Fagerberg, L., Hallstrom, B.M., Lindskog, C., Oksvold, P., Mardinoglu, A., Sivertsson, A., Kampf, C., Sjostedt, E., Asplund, A., et al. (2015). Proteomics. Tissue-based map of the human proteome. Science (New York, NY) 347, 1260419.
3. Kang, H.J., Kawasawa, Y.I., Cheng, F., Zhu, Y., Xu, X., Li, M., Sousa, A.M., Pletikos, M., Meyer, K.A., Sedmak, G., et al. (2011). Spatio-temporal transcriptome of the human brain. Nature 478, 483-489.
4. Pletikos, M., Sousa, A.M., Sedmak, G., Meyer, K.A., Zhu, Y., Cheng, F., Li, M., Kawasawa, Y.I., and Sestan, N. (2014). Temporal specification and bilaterality of human neocortical topographic gene expression. Neuron 81, 321-332.
5. Smith, C.M., Finger, J.H., Hayamizu, T.F., McCright, I.J., Xu, J., Berghout, J., Campbell, J., Corbani, L.E., Forthofer, K.L., Frost, P.J., et al. (2014). The mouse Gene Expression Database (GXD): 2014 update. Nucleic acids research 42, D818-824.
6. Szklarczyk, D., Franceschini, A., Wyder, S., Forslund, K., Heller, D., Huerta-Cepas, J., Simonovic, M., Roth, A., Santos, A., Tsafou, K.P., et al. (2015). STRING v10: protein-protein interaction networks, integrated over the tree of life. Nucleic acids research 43, D447-452.